Copyright Warning & Restrictions

The copyright law of the United States (Title 17, United States Code) governs the making of photocopies or other reproductions of copyrighted material.

Under certain conditions specified in the law, libraries and archives are authorized to furnish a photocopy or other reproduction. One of these specified conditions is that the photocopy or reproduction is not to be "used for any purpose other than private study, scholarship, or research." If a, user makes a request for, or later uses, a photocopy or reproduction for purposes in excess of "fair use" that user may be liable for copyright infringement,

This institution reserves the right to refuse to accept a copying order if, in its judgment, fulfillment of the order would involve violation of copyright law.

Please Note: The author retains the copyright while the New Jersey Institute of Technology reserves the right to distribute this thesis or dissertation

Printing note: If you do not wish to print this page, then select "Pages from: first page # to: last page #" on the print dialog screen

NJIT
New Jersey's Science & Technology University

The Van Houten library has removed some of the personal information and all signatures from the approval page and biographical sketches of theses and dissertations in order to protect the identity of NJIT graduates and faculty.

ELECTROLYTIC POLISHING OF COPPER AND NICKEL SILVER

BY

HALLE ABRAMS

A THESIS

PRESENTED IN PARTIAL FULFILLMENT OF

THE REQUIREMENTS FOR THE DEGREE

OF

MASTER OF SCIENCE IN CHEMICAL ENGINEERING

AT

NEWARK COLLEGE OF ENGINEERING

This thesis is to be used only with due regard to the rights of the author. Bibliographical references may be noted, but passages must not be copied without permission of the College and without credit being given in subsequent written or published work.

NEWARK, NEW JERSEY
1965

ABSTRACT

To facilitate the study of surface conditions on ultrasonic weldability, electrolytic polishing was used to obtain four types of surfaces on copper and nickel silver (alloy D). A 50% ortho-phosphoric acid bath was used, and the necessary operating conditions to obtain these surfaces were established. In accordance with current electrolytic polishing theory, the existence of the anode viscous layer and anode surface film was observed, and their role in the polishing process is discussed. By means of metallurgical techniques and surface profile measurements, it is shown that the four types of surfaces are significantly different, and good reproducibility of these surfaces are attainable. Statistical analysis of the data was employed to support the conclusions. As an outgrowth of this experiment, a method for deburring nickel silver contact springs has been established. Electrolytic polishing theory and a comprehensive literature survey relevant to this study are also presented.

Library
Newark College of Engineering
56140

APPROVAL OF THESIS

FOR

DEPARTMENT OF CHEMICAL ENGINEERING

NEWARK COLLEGE OF ENGINEERING

BY

FACULTY COMMITTEE

APPROVED: _____

_____

_____

NEWARK, NEW JERSEY

JUNE 1965

ACKNOWLEDGEMENTS

The author wishes to take this opportunity to express his appreciation to Dr. C. L. Mantell for his guidance and constructive criticism throughout the preparation of this manuscript, and to Mr. K. S. Stephens for assisting in the statistical analysis of the data.

TABLE OF CONTENTS

LIST OF FIGURES

LIST OF TABLES

I INTRODUCTION

A) Statement of the Problem and Introductory Remarks

In the electropolishing process the metal to be treated is the anode in an electrolytic cell, and depending on the conditions of operation and the solution used, the metal can be either etched, polished, pitted, or polished with some pitting. These surfaces are a function of the current density, which is affected to varying degrees by voltage, temperature, agitation, anode to cathode distance, concentration of electrolyte and anode to cathode surface area ratio. For a given set of parameters, if the anode current density versus voltage is plotted, you can obtain a curve consisting of four regions which correspond to the four types of surface finishes mentioned previously.

The object of this thesis was to determine the required electropolishing conditions to produce various surface finishes consistently, to enable a study of surface effects on ultrasonic weldability. Inherent to the electropolishing phenomena, various types of surface finishes can be obtained as described below. The distinguishing characteristics and identification of these surface finishes can be studied using profilometer measurements and standard metallographic procedures. These methods were employed in the present investigation and are discussed in more detail in the body of the thesis.

Although electrolytic polishing is commonly used in industry and research to obtain desired surface characteristics, the exact mechanism involved has not been established. Current theories attribute the observed phenomena of smoothing and brightening to the presence of a viscous layer of reaction products around the anode and to the formation of a thin film on the anode surface.

The smoothing action is controlled by the anode viscous layer. The presence of this layer was observed, and for the copper/orthophosphoric acid system, its formation as a function of time and voltage was studied. In the etching region, where no smoothing occurs, the anode viscous layer was not observed. For the copper orthophosphoric acid system, many investigators have attempted to determine the composition and properties of this layer. For instance, Halfawy[1] has identified the salt obtained by crystallization from the anode layer by its electron diffraction pattern as 4 $CuOP_2O_5H_2O$. Laforque-Kantzer[12] has suggested that the dissolved salt is of the type $PO_4(OH)CuH_2$.

The thin film on the anode surface controls the brightening action. The existence of this surface film has been demonstrated by various investigators. In the copper/orthophosphoric acid system, the brightening observed in the fast gas evolution region cannot be attributed solely to the anode viscous layer. In this region the viscous layer is continually forming and collapsing and therefore represents only a small part of the polishing mechanism.

In summary, the electropolishing process results from continued solution of the metal anode in such a way that irregularities on the surface are removed and the surface becomes smooth and bright, the chemistry of this anodic process being of a complex nature. A general discussion relating to electrolytic polishing is presented in the next section, and a literature review pertinent to this investigation is presented in section (IC). The remainder of the introductory section is devoted to a discussion of the equipment and procedure employed to obtain the experimental data. Section II pertains to the experimental observations and section III presents the associated statistical analysis of this data. The remaining sections of the thesis are the conclusions, further areas of study and the bibliography.

B) Electrolytic Polishing Theory

Electropolishing is an electrochemical process, the reverse of electroplating, whereby metal is removed instead of being deposited. An anodic viscous layer and surface film form during electropolishing when current is applied. Under proper conditions it is these effects which are believed to be primarily responsible for both the observed smoothing and brightening.

The examination of a metal surface reveals that on a microscopic scale the contour may be considered as a series of hills and valleys, the depth of the valleys and distances between the hills depending on the methods used to generate the surface. On a microscopic scale the surface is more complex, since smaller irregularities are superimposed on the macroscopic hills and valleys. In order to obtain a truly flat surface both the macroscopic and microscopic irregularitie must be removed. Thus the distinguishing functions of an ideal polishing process are smoothing, that is the elimination of the large scale irregularities (above one micron in size) and brightening, that is the removal of the smaller irregularities (down to about 1/200 micron is size). Consequently, leveling of the coarse projections is called macropolishing, which is synonymous with smoothing, and the dissolution of the microscopic irregularities is referred to as micropolishing which is synonymous with brightening. Thus, when macro- and micropolishing occur simultaneously, both smoothing and brightening are observed. In certain instances, either can occur independently of the other. However, as mentioned previously, the

feature of an electropolishing process is that it combines both functions.

Any complete theory of the mechanism of electropolishing must explain both the smoothing and brightening of the metal surface. Present theories attribute these effects to two distinct but related processes. They are the presence of a viscous layer of reaction products around the anode and the formation of a thin film on the anode surface. The existence of the anode viscous layer and the anode surface film and the observations made by other researchers are discussed in the next section, (IC). The present discussion will be of a general nature, the purpose being to introduce these theoretical concepts and show how they fit into the overall scheme of an electrolytic polishing operation.

Electron diffraction studies have indicated that during electropolishing, an oxide (or hydroxide) film is formed by electrolytic oxidation at the anode. This anode film covers the metal surface being polished and is believed to be responsible for macro-polishing, (see figure 1). The extreme portion of the layer continuously dissolves into electrolyte, and during electropolishing suitable conditions are established which maintains a constant anodic film thickness. This equilibrium between the oxide formation on one side and the rate of chemical dissolution into the electrolyte on the other, allows the electron exchange between the metal being polished and the ions of the electrolyte. If, as various experimenter's results suggest,[3] the rate determining process during polishing is one of

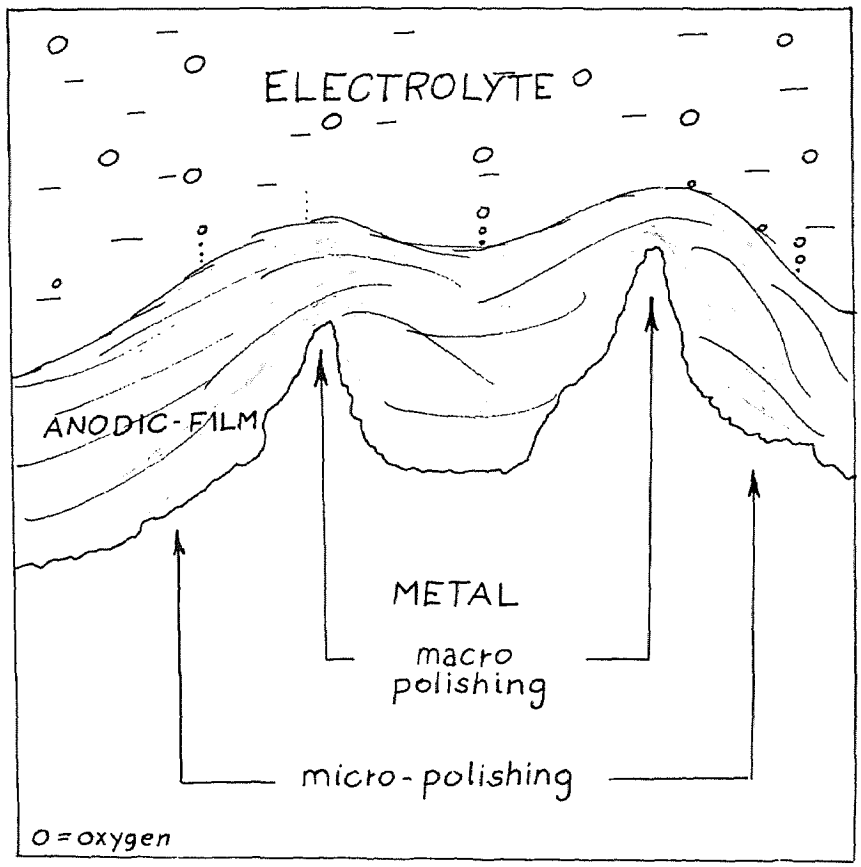

Figure 1. Schematic of electropolishing mechanism.

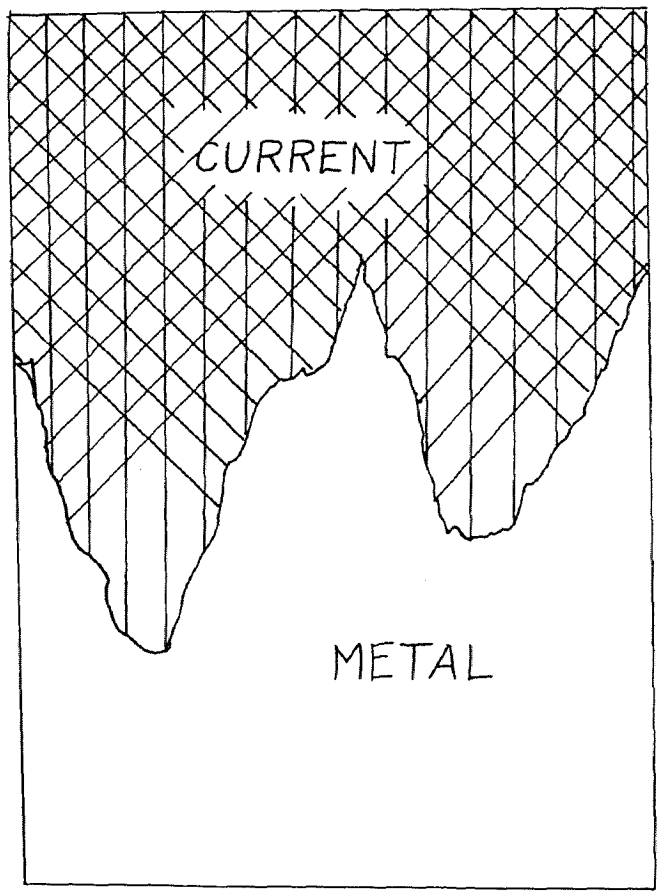

Figure 2. Schematic of current distribution on irregularities during electropolishing.

diffusion in the viscous layer, then the viscous layer controls the rate of dissolution of the anode by controlling the rate at which the products of the anodic dissolution can diffuse away. Consequently, the smoothing or macro-polishing can be accounted for qualitatively by the differences in the concentration gradient over the peaks and valleys of the metal surface. Referring once again to figure 1, it can be seen that at the peaks the anodic film is thin and thus the concentration gradient is high, while in the valleys the film is thicker and the concentration gradient is lower. Thus, preferential dissolution of the peaks occur, and the surface is smoothed. Another qualitative aspect of the smoothing phenomena is that a greater area is exposed on the projections, which are therefore subject to greater current densities, thereby increasing the rate of anodic dissolution, (figure 2).

While the concept of the anode viscous layer can account for the smoothing process, it does not adequately explain the electrolytic polishing process, since the observed brightening must also be resolved. A complete discussion of this phenomenon is presented in the next section. In the present discussion, I would simply reiterate that the formation of a thin film on the surface of the anode is responsible for the brightening action. With this basic background on electropolishing theory, a more rigorous presentation can be made in the literature survey section of the thesis.

C) Literature Survey

The literature review comprising this section of the thesis has been broken down into three subsections for clarity and ease of presentation. These subsections are; the relation between anode potential and anode current density, an amplification of the anode viscous layer and anode surface film concepts, and the effects of various parameters on the electropolishing process.

The relation between anode potential and anode current density can best be explained by considering a simple electrolytic cell consisting of two electrodes, an electrolyte and an external potential source. To remain consistent with the information contained in figure 3, which is reproduced from Tegart,[3] assume for the present discussion that a potentiometric circuit is used as the external potential source. If an increasing potential is now applied across the cell, and the cell is allowed to reach equilibrium at each voltage change, then the anode potential, the cathode potential and the voltage drop across the cell will be related to the anode current density approximately as shown in figure 3. These curves are characteristic of those obtained in cells where a limiting current is produced by concentration over-potential. Further the considerable drop in current from B to C is characteristic of the onset of some passivity process. However, in adherence to the strict definition of passivity, since the metal still dissolves at an appreciable rate, this current drop is due to only partial passivity.

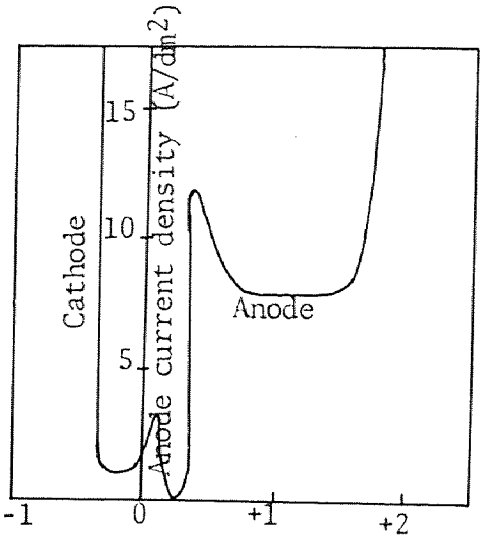

(a)

Potential refered to standard hydrogen electrode (V).

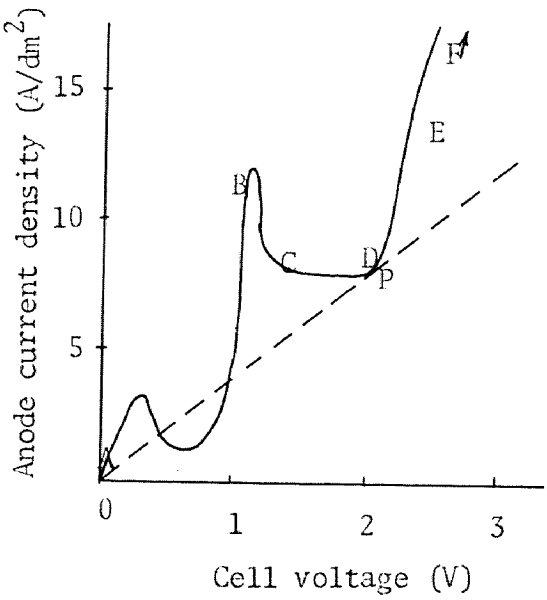

(b)

Figure 3. Curves of anode potential, cathode potential and cell voltage as functions of anode current density for copper in 900 g/l orthophosphoric acid (potentiometric circuit). The regions on the cell voltage curve can be distinguished as: A-B etching; B-C unstable; C-D stable plateau with polishing; D-E slow gas evolution with pitting; E-F polishing with rapid gas evolution.

Under such conditions of partial passivity it is reasonable to expect the values of voltage and current density for any given portion of the curves to vary, depending upon the manner in which the voltage is applied to the cell. However, the form of the curves will remain the same. Referring once again to figure 3b, the surface finishes mentioned previously can be related to specific sections of this curve. Along AB the specimen is etched; at BC instability occurs, and periodic oscillations of current density may occur; along CD polishing occurs; along DE the surface becomes pitted; and at higher voltages, point F and above, a polished and pitted surface finish is obtained. The experimental results for copper and nickel silver agree very well with this general curve, and a more complete discussion of this aspect of the investigation is presented in section II.

Mention has been made to the presence of the anode viscous layer and anode surface film. Consideration will now be given to the existence of these layers and the role they play in the electropolishing process. The anode viscous layer has been observed by various investigators for a variety of electropolishing systems. Microscopic examination shows that in the region of constant current density i.e. along CD in figure 3b, the surface of the anode becomes covered with a viscous layer which tends to stream off during the polishing operation. In certain systems the anode viscous layer is visible, i.e. when the electrolyte is colorless and the products of solution are highly colored. In the Cu/orthophosphoric acid

system, if a fresh electrolyte which is colorless is used, the anode viscous layer can be observed, since the reaction products are colored blue. P. A. Jacquet[4] microscopically observed the viscous layer for the Cu/orthophosphoric acid system and found that at the outer limit of the anode viscous layer there is an approximately planar interface between the layer and the bulk of the solution. He also observed that this layer formed from the point B (figure 3b) onwards, and reached a constant maximum thickness of about .005 cm. along the plateau CD. It is interesting to note that this layer is not observed for conditions corresponding to the region AB in figure 3b, the etching region. Thus it can be concluded that since the layer is of constant thickness along the polishing plateau, the associated increase in resistance of the cell between the points B and D is related to this layer of electrolyte rich in dissolved metal and that this layer plays a part in the mechanism of polishing. Further evidence of the role the anode viscous layer plays in the polishing process has been reported by H. F. Walton.[5] He used a copper specimen in the form of a horizontal disc as the anode, and rotated it rapidly in an orthophosphoric acid solution. When the speed of rotation was sufficiently high, only the center of the disc was polished, while outside this area etching occurred. This was attributed to the linear velocity being so great that turbulence was set up and the viscous layer could not form at the extremities of the disc. When the cell voltage was raised, thus increasing the rate of solution of the metal, the zone of polishing

was extended. Walton attempted to obtain the composition of the anode viscous layer, however because of its complex chemical nature and because of the difficulties in sampling his results were necessarily qualitative. He reported that the anode viscous layer consisted of a supersaturated solution of copper phosphate in which the high concentration of copper leads to a marked increase in viscosity. Subsequent investigations of the anode viscous layer with more sophisticated techniques have yielded quantitative results. For example, Halfawy [1,6] reported that the salt obtained by crystallization from the anode viscous layer has been identified by means of its electron diffraction pattern as $4(CuO.P_2O_5.H_2O)$. A possible criticism is that this formula does not necessarily represent the compound in solution. Laforque-Kantzer[2] has shown, by infra-red spectrography of the layer itself, the occurrence of free and combined hydroxyl ions, and suggests on the basis of chemical and acidimetric analysis, that the dissolved salt is of the type $PO_4(OH)CuH_2$. However, regardless of the composition of the viscous layer, it has been shown that there is a correlation between the polishing observed and the presence of the anode viscous layer. Based on the above literature review, it has been shown that the concept of the anode viscous layer is a real entity and not a theory proposed by a prominent electrochemist. Utilizing this premise a mechanism of electropolishing may now be proposed which will account for the observed smoothing and brightening. However, before discussing a polishing mechanism it is more

appropriate to consider the anode surface film and its role in the polishing process.

Walton[5] showed that the conductivity of the viscous layer for the Cu/orthophosphoric acid system was approximately 2×10^{-2} $ohm^{-1}cm^{-1}$. This results in a resistance for the layer of 2.5 ohm/cm^2, for a thickness of .05 cm. However, the resistance for this system varies between 10 to 23 ohm/cm^2 along the plateau, thus the viscous layer contributes only a tenth to a quarter of the observed resistance. It is therefore clear that some additional factor is involved, and there is now considerable evidence suggesting that the formation of some sort of film on the anode surface plays an important role in the polishing process. Hoar and Farthing[7] studied the wetting of a copper surface by mercury under conditions of etching and polishing in orthophosphoric acid. In the etching region the mercury wet the surface, whereas in the polishing region it failed to do so. This absence of wetting was attributed to the existence of a surface film, which is consistent with the fact that mercury will not wet a copper specimen that has been heated in air so as to produce a thin oxide film. Additional evidence of the anode surface film was reported by Meunier,[3,8] who studied the periodic oscillations of current and voltage which usually occurs in the unstable region of the anode current density vs. voltage curve (region BC in figure 3b). He concluded that the observed periodic oscillations were due to the periodic growth and destruction of a thin oxide film on the surface of the anode. It should

be noted that this film appears more readily on a surface which has been prepared by abrasion. This was the case for the present experiment, and the periodic oscillations in the unstable region were clearly evident.

Direct experimental evidence for the existence of the anode surface film is difficult to obtain. Since the film is so thin, it usually dissolves during removal of the anode from the cell, or if a film is noted, it may have formed by oxidation of the polished surface on exposure to the atmosphere. However, indirect evidence for the existence of the anode surface film can be obtained by studying the decay of the anode potential when the applied voltage is cut off after polishing. H. Lal[9] performed studies of this nature for the Cu/orthophosphoric acid system, and found that the electrode potentials immediately after cut off were more positive then the reversible oxide potentials. He attributed this behavior to a special type of surface oxide with properties different from those of a bulk oxide, and suggested that the interface consisted of adsorbed oxygen and/or a thin surface oxide film. Lal also observed a distinct difference between polishing and non-polishing systems. Namely, when polishing was observed, the potential decay period was short, approximately a twentieth of a second. In non-polishing systems the decay period was long and varied from several seconds to minutes. Assuming that there is a relation between the potential decay period and the thickness of the anode surface film present during polishing, these observations suggest that the anode

film is extremely thin, probably only a few atomic layers thick. Therefore, it is likely that the film undergoes a continuous process involving dissolution by the electrolyte and renewal by metal from the anode. The presence of the anode surface film can be used to explain the brightening which is observed in cases where copious gas evolution occurs (e. g. at high current densities, region EF in figure 3b). Under these conditions the anode viscous layer exerts little influence, since it is continually breaking down and regenerating and does not attain a steady state condition. The existence of this extremely thin anode surface film also provides an explanation for the difference between etching and brightening conditions. If the electrolyte has free access to the surface of the anode, etching results because dissolution of the metal occurs preferentially from sites of higher energy (e. g. grain boundaries). However, to obtain a bright surface, such preferential attack must be prevented, enabling dissolution of the microscopic irregularities as discussed in section IB. This is the role of the anode surface film, to act as a barrier to preferential attack of the anode. Although the exact role of the surface film is uncertain, a qualitative explanation has been proposed. Assuming the film follows the contours of the surface and is attacked uniformly by the electrolyte, to maintain the film, the passage of metal ions across the metal-film interface must occur at the same rate at all points. This causes brightening, since such uniform removal of metal from a surface will dissolve the microscope irregularities.

Now that the evidence and the role played by the anode viscous layer and anode surface film have been explained, we may direct our attention to the statement of an electropolishing mechanism. The proposed mechanism must be consistent with the roles of the anode viscous layer and anode surface film and must be of a general nature. Consequently, the mechanism which fulfills these requirements appears to be the diffusion mechanism. This mechanism as applied to the anode viscous layer, resulting in smoothing or macro-polishing was discussed in section IB. In brief, the ions of the metal are dispersed from the anode by diffusion in the viscous layer. Since the rate of solution at any point on the surface is determined by the concentration gradient, as described in section IB, the asperities will be dissolved first. The basic diffusion mechanism as presented above was originally stated by Elmore.[10,11] This basic approach must be modified somewhat to explain micropolishing. Halfawy[6] has proposed a theory of polishing different from that of Elmore. He suggested that it was not so much the diffusion of metallic ions that controlled the dissolution of the metal, but the distribution of the anions over the asperities and depressions on the anode, under the action of the electric field and viscosity. Edwards[12] developed this concept into the Acceptor Theory. Using an extremely sophisticated technique, he showed that the change in the macroprofile of copper during polishing in phosphoric acid is comparable with that deduced theoretically on the basis of the primary distribution of the current, the dissolution being entirely

controlled by diffusion.[13] Wagner[14] performed a mathmetical analysis of an ideal electropolishing process, based on a mechanism of diffusion of the acceptors, and the macroprofile deduced from his analysis agreed with Edward's observations. This analysis also lead to the conclusion that the smallest asperities disappeared first, i.e. micropolishing precedes macropolishing. Considerable evidence has been gathered which attributes the observed micropolishing to the existence of a thin anode surface film. The diffusion mechanism of electropolishing involving the transistory formation of a thin solid film is consistent with Edward's theory of acceptors. The anode viscous layer serving as a screen for the arrival of acceptors at the surface is still the fundamental concept. The presence of a thin anode film of salt crystallizing from such a layer, rich in the products of solution, or the discharge hydroxyl ions leading to the formation of oxides are secondary reactions, which play an important role in the observed micropolishing.

Other theories have been proposed to explain the electropolishing process. The Passivation Theory of U. R. Evans[15] was based on the passivation of the depressions in the anode surface. The Ionic Adsorption Theory of Darmois[16] and his collaborators involved the adsorption on the anode of the anions present in the electrolyte. Other theories which have found little support are those of Yozdvizhensky,[17] Mercadie[18] and Knuth-Winderfeldt.[19]

The literature associated with the anode viscous layer and

anode surface film concepts have been reviewed and related to a general electropolishing mechanism. A further literature survey deals with the more practical aspects of electropolishing theory, namely the effects of various parameters on the electropolishing process, primarily with the Cu/orthophosphoric acid system.

One of the factors considered by previous investigators is temperature. In general the resistance of an electrolyte decreases with increasing temperature, and thus the voltage required to give the same current density is less, per Ohm's Law. It has been found empirically[20] that the voltage, V, required to maintain a given current density is given by the equation,

$$V=K/(a\theta + b)$$

where θ is the temperature, and K, a and b are constants determined by the conductivity of the electrolyte, the dimensions of the cell and the current passing through the cell. From this equation it is seen that as the temperature increases the power required to maintain a given current density is lowered, indicating for economy use higher temperatures. However, at high temperatures the viscosity of the bath decreases, making it more difficult to maintain the anode viscous layer. Thus, the effective operating temperature, must be a compromise between conflicting effects.

Honeycombe and Hughen[21] determined the relation between anode potential and current density at various temperatures for an electrolyte containing 522 grams/liter of orthoposphoric acid. At each

temperature the length of the polishing plateau was the same, but the plateau occurred at different current densities. As the temperature was increased the limiting current density also increased, but at the higher current densities the polish became uneven. Hickling & Higgens[22] found little change in the limiting current density for a dilute orthophosphoric acid electrolyte (98 grams/liter), when the temperature was increased from 20 to 70 degrees C. However, in more concentrated solutions the current density increased rapidly with temperature, e.g. with 784 grams/liter orthophosphoric acid the limiting current density at 50° C was 2.5 times the value at 20° C. This figure agrees with the results of Honeycombe and Hugen who noted an increase in current density of about 2.2 times when the temperature was raised from 22° C to 50° C for a 522 gram/liter orthophosphoric acid electrolyte.

Another parameter which will effect the polishing process is the concentration of the electrolyte. Honeycombe and Hughen[21] determined the relation between anode potential and current density at room temperature for a range of concentrations of orthophosphoric acid from 65 to 1570 grams/liter. They found that the polishing plateau occurred over approximately the same range of voltages, but the limiting current density varied with the concentration. The curve of limiting current density versus concentration of electrolyte showed a maximum at a concentration of about 300 grams/liter. For each concentration of electrolyte, a copper specimen was polished for ten minutes at a voltage corresponding to the

middle of the polishing plateau and the surface finish was noted. The most satisfactory, uniform polish occurred at a concentration of 522 grams/liter, the limiting current density being 3.88 A/dm^2.

Some qualitative results have been reported by Hickling and Higgens[22] on the effect of viscosity on the polishing process. They found that the limiting current density was inversely proportional to the viscosity for othophosphoric acid solutions containing varying amounts of glycerol. Because the three variables, temperature, concentration and viscosity have an effect on each other, this interaction or confounding makes it difficult to study the effect of these parameters on the polishing process.

Another parameter which effects the polishing process is agitation of the electrolyte. During electrolytic polishing under steady state conditions, the reaction products tend to accumulate about the anode. In some cases, diffusion and convection cannot supply sufficient fresh electrolyte to the anode, and agitation is required to remove some of the reaction products and maintain the viscous layer at the optimum thickness for polishing. However, excessive agitation can prevent the formation of the viscous layer and thus polishing would not be achieved. Hickling and Higgens[22] found that mechanical stirring increased the limiting current density by a factor of 3 to 5 times. In many cases the best results are obtained by rotating or oscillating the anode, rather than by agitating the electrolyte. However, since higher current densities are re-

quired for a moving anode in order to maintain the viscous layer, and since an additional variable is introduced, if satisfactory results are obtainable without agitation, then this variable should be excluded from the procedure.

Other factors which must be considered are the initial surface preparation, time of treatment, size of electropolishing system, anode to cathode surface area ratio and anode to cathode spacing. In general the polishing time decreases with increasing fineness of the initial finish. However, the uniform current density and lack of concentration gradients on a smooth surface may result in a relatively slow increase in metal ion concentration around the anode, and thus the establishment of polishing ocnditions may require a longer time with a smooth surface than a rough surface. If the initial finish is too rough, the time required to produce a smooth surface is long, and the amount of metal removed is excessive. Generally it is good practice in a laboratory type experiment to mechanically polish all of the test coupons the same way, to eliminate this parameter from effecting the experimental results. Besides the initial state of the surface, the metal and the electrolyte utilized also influence the time necessary to obtain a given polish. However, as an approximate general rule it has been found that the time of treatment is inversely proportional to the current density. This experimenter noted that for a given current density there was an optimum time for the best polish and treatment for longer times resulted in a poorer surface finish. The anode to cathode surface

area ratio affects the voltage range over which the polishing plateau exists. The present study indicated that for an anode to cathode ratio of approximately 1:1, the polishing plateau was not clearly defined. However, by increasing the cathode to anode surface ratio to 1.65:1, the polishing plateau extended over a 1 volt range. Similar results were reported by Honeycombe and Hugan[21]. The effect of anode to cathode spacing shows up in the limiting current density, since this spacing influences the internal resistance of the cell. With regards to industrial applications of electrolytic polishing, an important factor is the size of the system. Because changes in the size of the system cause considerable changes in the operating conditions, many times the electrolyte used for an industrial application differs from that used to polish the same metal on a laboratory scale. Agar and Hoar[23] have shown that for two cells A & B which differ only in size, to be equivalent the ratio 1/K must be constant. That is, for the current densities and potentials in both cases to be the same at all corresponding points in the two cells, the length of line joining two corresponding points on the electrodes in the cells (1) and the specific conductivity (K) in the ratio 1/K must be constant. Thus K must be altered for any change in 1.

ID) Procedure and Equipment

A literature search revealed that considerable work had been done on the Cu/H_3PO_4 system. Consequently, orthophosphoric acid was used to study electropolishing of copper. Certain parameters were held constant (temperature and degree of agitation) while cell voltage, concentration, anode to cathode distance, and anode to cathode surface area ratio were varied. Concentration changes influence the polishing process, because of the dependence of current density on this parameter. A 50% H_3PO_4 solution was found to yield the desired results. To facilitate adjustments of the bath and maintain this concentration, specific gravity measurements were taken periodically. The data shown in figure 4 indicates that the concentration of the bath can be obtained by performing specific gravity measurements. The anode to cathode surface area ratio affects the voltage range over which the polishing plateau exists. When the anode to cathode ratio is approximately 1:1, the polishing plateau is not clearly defined (Figure 7). By increasing the cathode to anode surface area ratio to 1.65:1, the polishing plateau extended over a 1 volt range (Figure 6). Similar results were obtained by Honeycombe and Hughan (1,21). Considerable sludge build-up was obtained on the copper cathode of the electrolytic cell. By increasing the cathode to anode surface ratio, this problem was made less severe. Masking the back of the cathode with a vinyl spray also helped to minimize this problem.

Figure 4. Specific Gravity vs. Concentration H_3PO_4

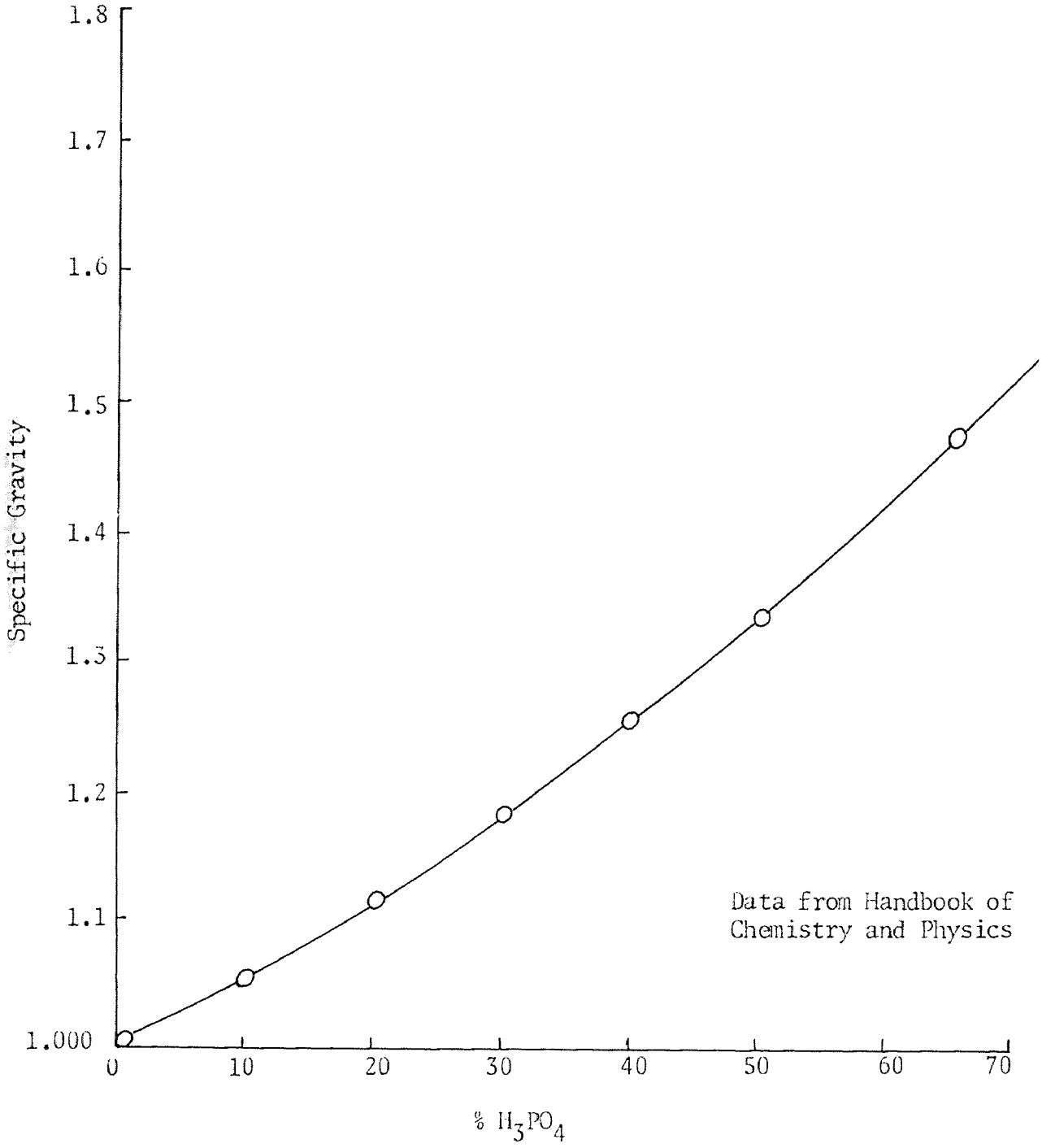

The final parameters used for treating copper were: 50% orthophosphoric acid (sp. gr. = 1.335); room temperature; no agitation or oscillation of either electrode; 1-1/2" electrode spacing; anode to cathode surface ratio of 1:1.65; varying the voltage from 1 to 7.8 volts. The experimental procedure consisted of mechanically removing the oxide from the surface using 600 grit paper and ultrasonic cleaning of the surface with trichloroethylene. The polishing bath has to be "broken in", by operating at low voltages for about two hours.

The surfaces obtained were examined metallographically, and to obtain quantitative data, thereby enabling a statistical analysis of the results, surface profile measurements were made using a Talysurf Profilometer. Typical Talysurf traces and the associated data are presented in figures 8 and 9, for four samples, one from each region on the anode current density vs. voltage curve. The thickness of material removed for these four samples was obtained by the weigh, process, reweigh technique.

A similar procedure to that mentioned above was followed to determine the operating conditions required to obtain the four types of surface finishes using a nickel silver anode. The final choice of using a 50% orthophosphoric acid bath, instead of those baths recommended in the literature, is discussed in a later section of this report.

The equipment used to perform the experiment was standard for electropolishing studies. A selenium rectifier was used as the power supply, and it was connected in a potentiometric circuit as shown schematically in figure 5. Oxygen free high conductivity copper was used as the electrodes, and a plexiglass fixture was designed and built to facilitate the handling of the copper and nickel silver coupons. Reagent grade orthophosphoric acid was used as the electrolyte, and a standard battery jar accommodated the electrolyte and electrodes. A standard ammeter and voltmeter was employed to measure the current and voltage. Metallographic studies were made with a Leitz Metallograph and the profile measurements with a Talysurf (model 3) Profilometer.

Figure 5. Schematic of experimental set-up.

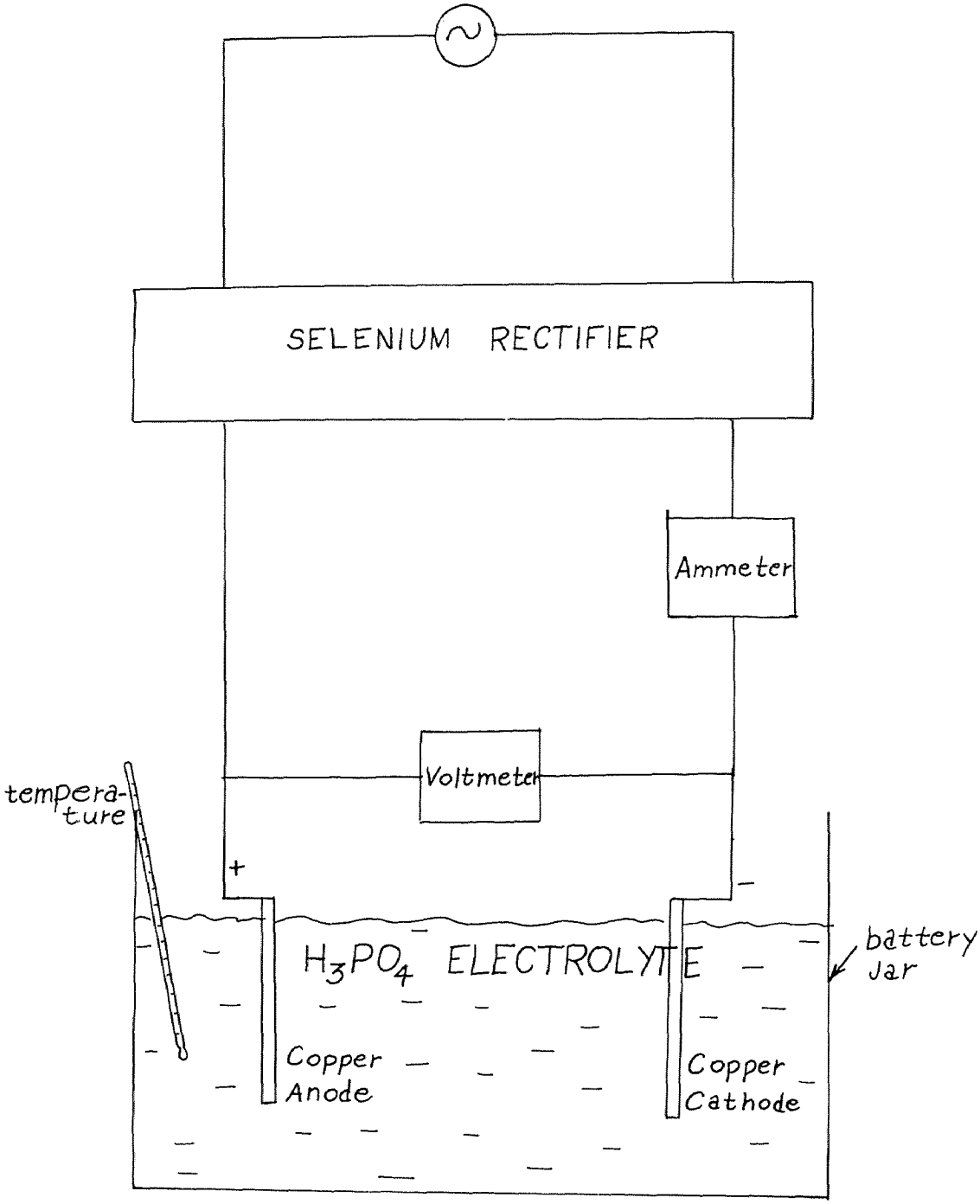

II) EXPERIMENTAL OBSERVATIONS

A) Electropolishing of Copper

The introductory section of the thesis has provided the theoretical background and discussed the procedure followed to obtain the data to be discussed in this section. The discussion relating to the electropolishing of copper will be broken up into three segments: Metallurgical examination of the surfaces and its relationship to the anode current density vs. voltage curve; Talysurf Profilometer measurements; Observations pertinent to the anode viscous layer.

1) Metallurgical examination of the surfaces. As mentioned previously, all of the coupons processed were metallurgically examined with a Leitz Metallograph. With reference to figure 6, it is seen that changes in the surface condition during treatment can be related to specific sections of the anode current density vs. voltage curve. The data for curves 6 and 7 are given in Tables I and II on pages 39 and 40 . From A-B is called the etching region; the micrograph shows the structure of the copper, which was cold worked as indicated by the small grain size. Copper oxide impurities are also present. This treatment removes approximately .0004 inches of metal in 300 seconds. The surface has a dull, satin finish, indicating the anode viscous layer does not form in this region. From B-C is the unstable region, characterized by periodic oscillations of current and voltage. These periodic

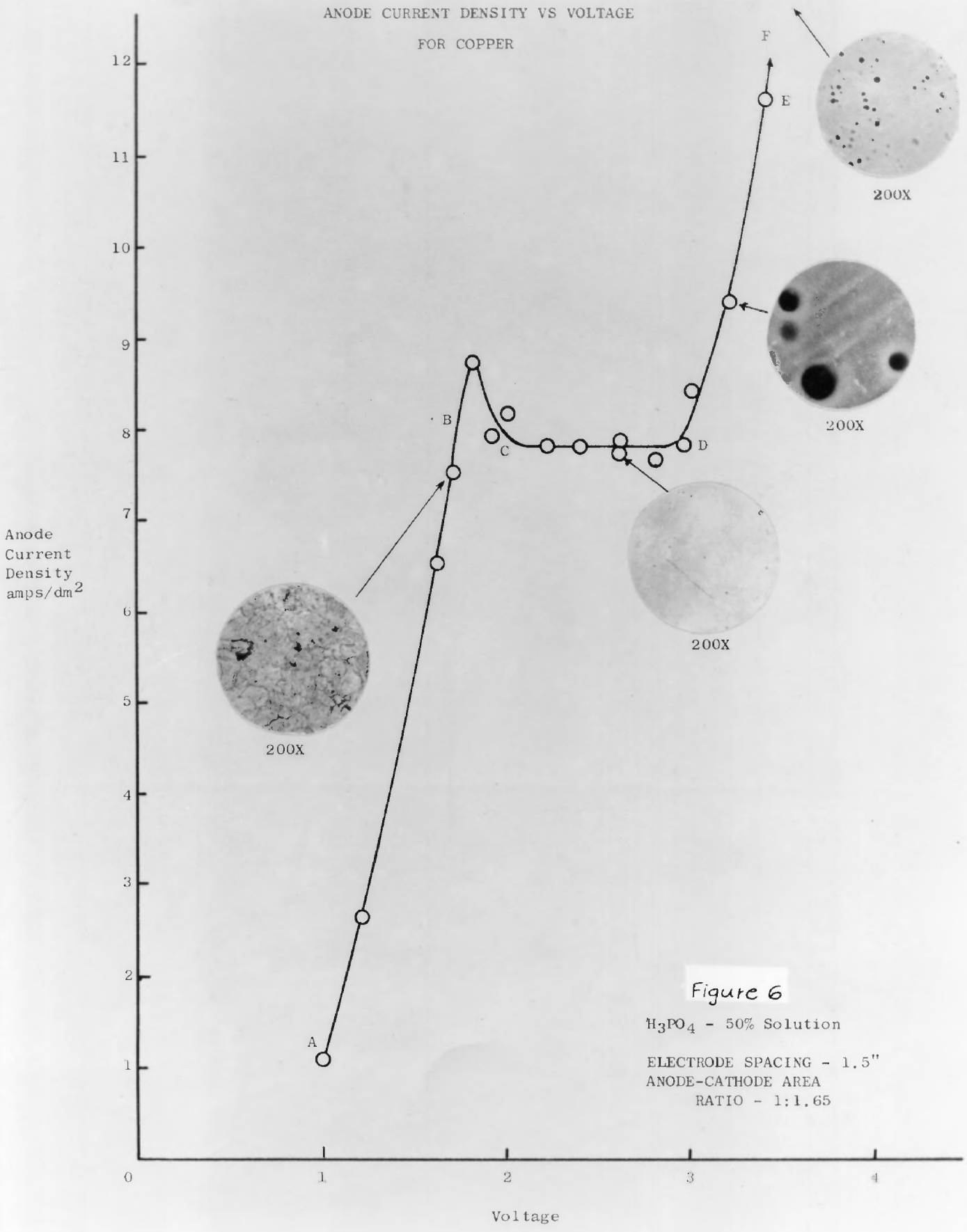

Figure 6

H_3PO_4 - 50% Solution

ELECTRODE SPACING - 1.5"
ANODE-CATHODE AREA
RATIO - 1:1.65

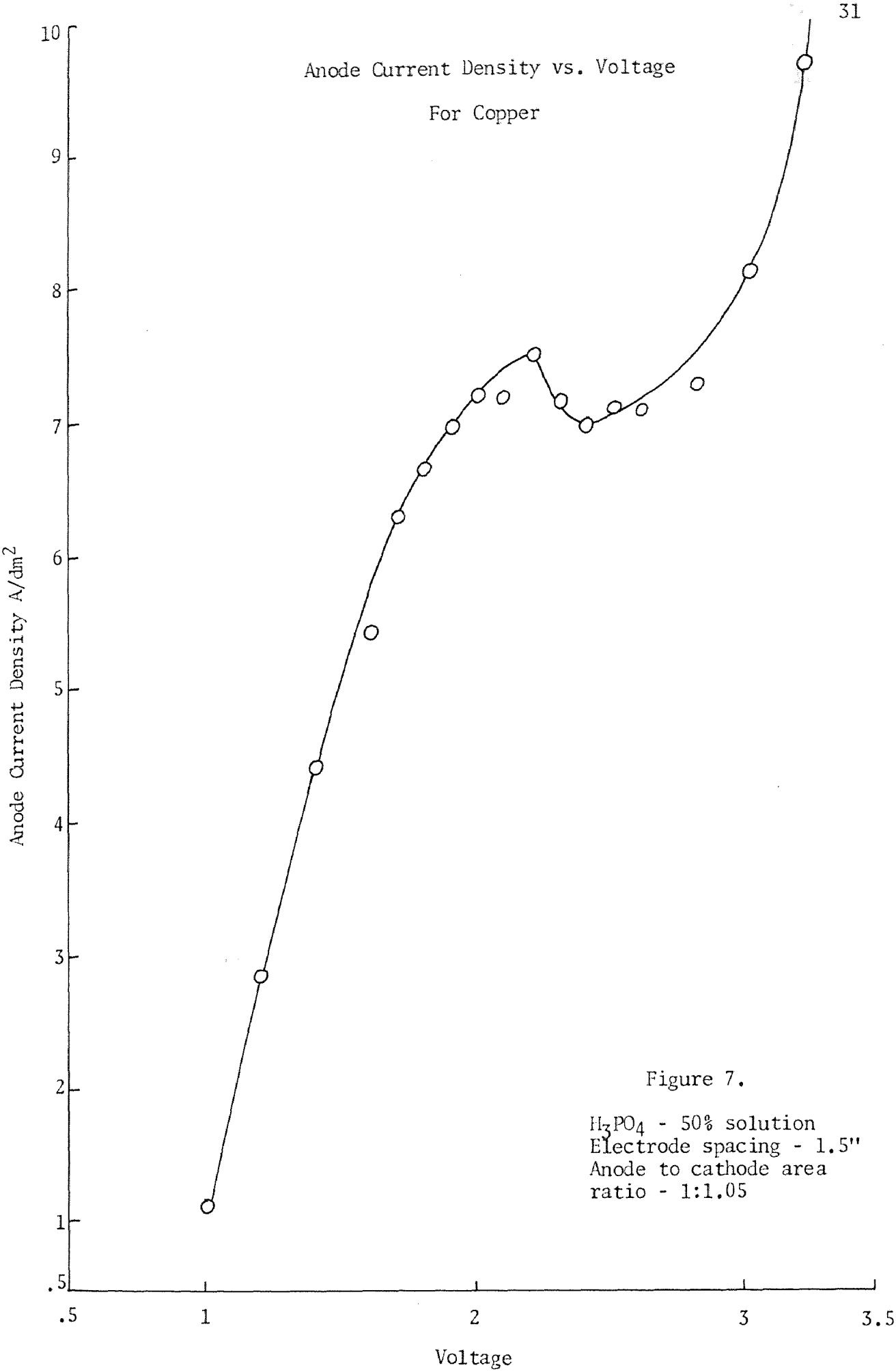

Figure 7.

H_3PO_4 - 50% solution
Electrode spacing - 1.5"
Anode to cathode area ratio - 1:1.05

oscillations that occur before polishing conditions are established have been attributed to cycles of passivation and activation.[24] For both the copper and the nickel silver systems these oscillations were observed. The region from C-D is the polishing plateau, characterized by a constant current density (called the limiting current density). The micrograph shows the smooth surface associated with this region; the black spots are oxide impurities observed previously. At these conditions about .0007 inches of metal is removed in 500 seconds. The anode viscous layer forms from point C onwards, and according to Jacquet,[1] reaches a constant maximum thickness of about .005 cm. along the plateau CD. Along D-E exists the slow gas evolution region, which results in a pitted surface consisting of many "hills and valleys". About .0006 inches of metal is removed in 300 seconds. Beginning at point D, oxygen is liberated at the anode, and the bubbles adhere to the surface and produce relief effects; the metal is still brilliant though rough.

The liberation of gas becomes increasingly vigorous along the branch of the curve, DE, giving way to the fast gas evolution region from E-F. At very high current densities, in the fast gas evolution region, a good polish can again be obtained. The micrograph shown is for a specimen treated at 6.0 volts and a current density of 45.2 amps/dm^2, resulting in a smooth but slightly pitted surface. At these conditions .0011 inches of metal was removed in 300 seconds.

The curve in Figure 6 was separated into three portions and a

regression analysis using the method of least squares was used to get the "best fit" model for the data obtained. In the etching region, a complex polynomial model is required to fit the curve and explain the blip (unstable region) predicted by the current electropolishing theory. On the polishing plateau the simple model $Y=\bar{Y} = 7.81$ was the best fit model. In the gas evolution region a quadratic regression model, $Y = -16.84 + 7.05X + 0.424X^2$ gave the best fit. The details of the curve fitting are presented in section III of the thesis.

2) Talysurf profilometer measurements. Referring to the data in table I, run III, the indicated coupons, namely samples F, M, R, and U were selected as representative of the surface finishes obtained over the four regions of the anode current density vs. voltage curve as shown in figure 6. To determine if there were significant differences between the four types of surfaces, and if it were possible to consistently produce these surfaces, a test yielding quantitative data was required. As a result, the surfaces produced were evaluated with a Talysurf, a sensitive device for measuring surface profiles. Five specimens for each of the four regions were prepared, and typical Talysurf traces and the associated data are presented in figures 8 and 9. By means of various statistical techniques, such as the Runs Test, t Test, and $\bar{X}$ and R chart, it was concluded that: there was good consistency among samples given the same treatment; four different populations existed (i.e. the surfaces obtained from each of the

Talysurf Traces For Copper

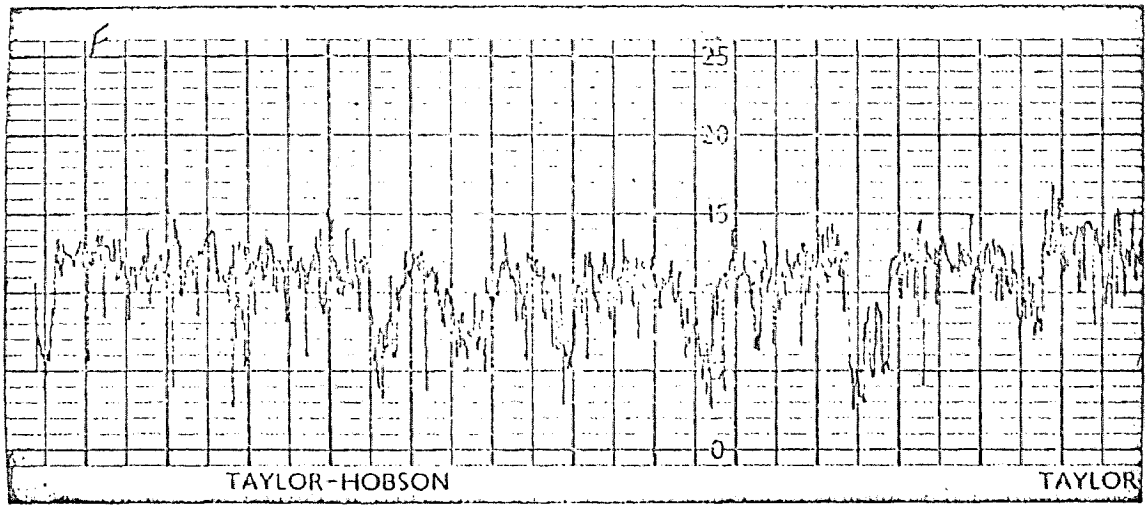

Etching region

Sample III F
4000 Å/division
$\bar{X}$ = 13,200 Å
S = 7320 Å

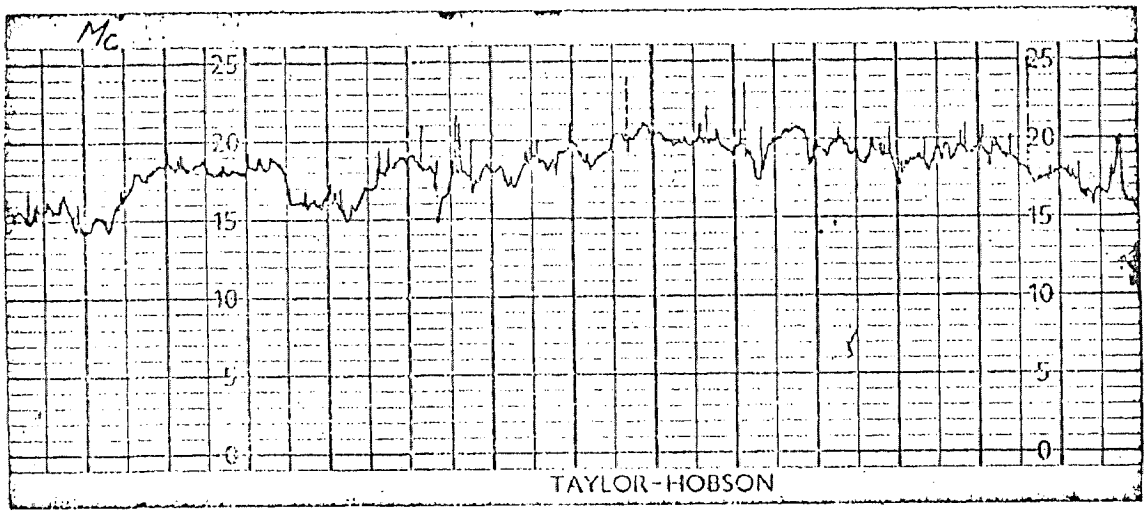

Polishing Plateau

Sample III M_c
1,000 Å/division
$\bar{X}$ = 1300 Å
S = 710 Å

Figure 8. Talysurf traces for copper, etching region and polishing plateau.

Talysurf Traces For Copper

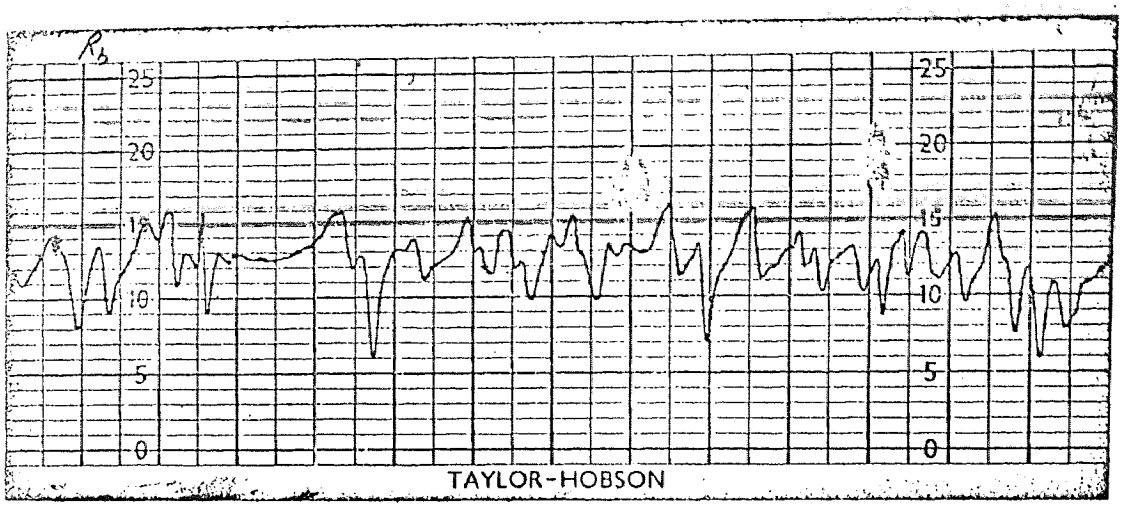

Slow gas evolution region

Sample III R_b
10,000 Å/division
$\bar{X}$ = 36,000 Å
S = 23,800 Å

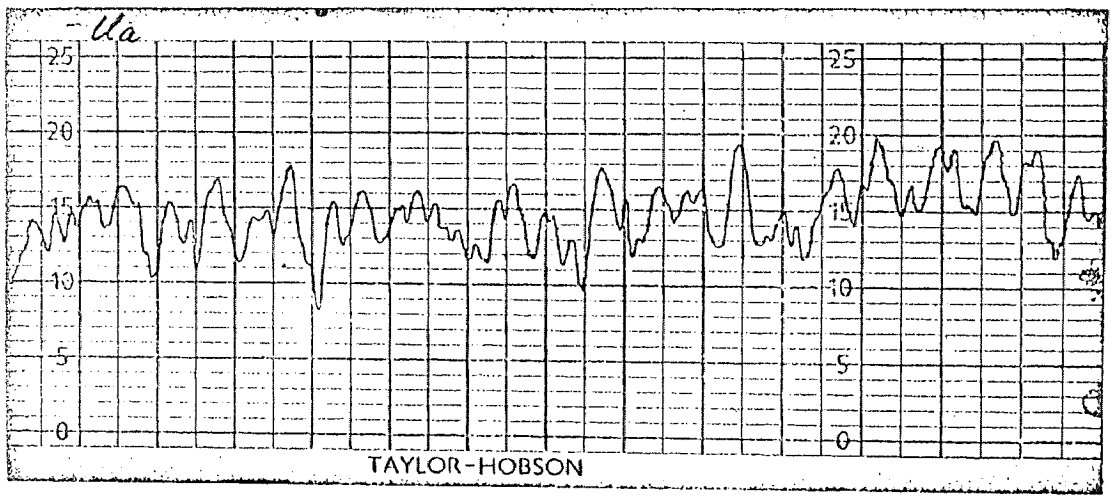

Fast gas evolution region

Sample III U_a
4000 Å/division
$\bar{X}$ = 10,000 Å
S = 6400 Å

Figure 9. Talysurf traces for copper, slow and fast gas evolution regions.

four regions on the current density vs. voltage curve were significantly different). The details of the above mentioned statistical analysis are discussed in section III.

3) Observations pertinent to the anode viscous layer. The existence of the anode viscous layer, and its role in the polishing process has been discussed in detail in section I. The purpose of this section is to present quantitative data for the time required to form this layer at various voltages, specifically over the polishing plateau and in the slow gas evolution region. Figure 10 is a plot of anode current density vs. time, in the Cu/H_3PO_4 system, for various voltages along the polishing plateau. It takes about 200 seconds for the anode viscous layer to form, after which smoothing occurs. As would be expected along the polishing plateau, all of the curves level off at approximately the same current density; that is, the limiting current density for the specific conditions of the run. Figure 11 is a plot of anode current density vs. time, in the slow gas evolution region, for the Cu/H_3PO_4 system. As the voltage increases, the anode viscous layer forms more rapidly and the limiting current density increases. In the region of fast gas evolution, the anode viscous layer forms almost instantly, but then breaks up, resulting in a cyclic process of forming and collapsing.

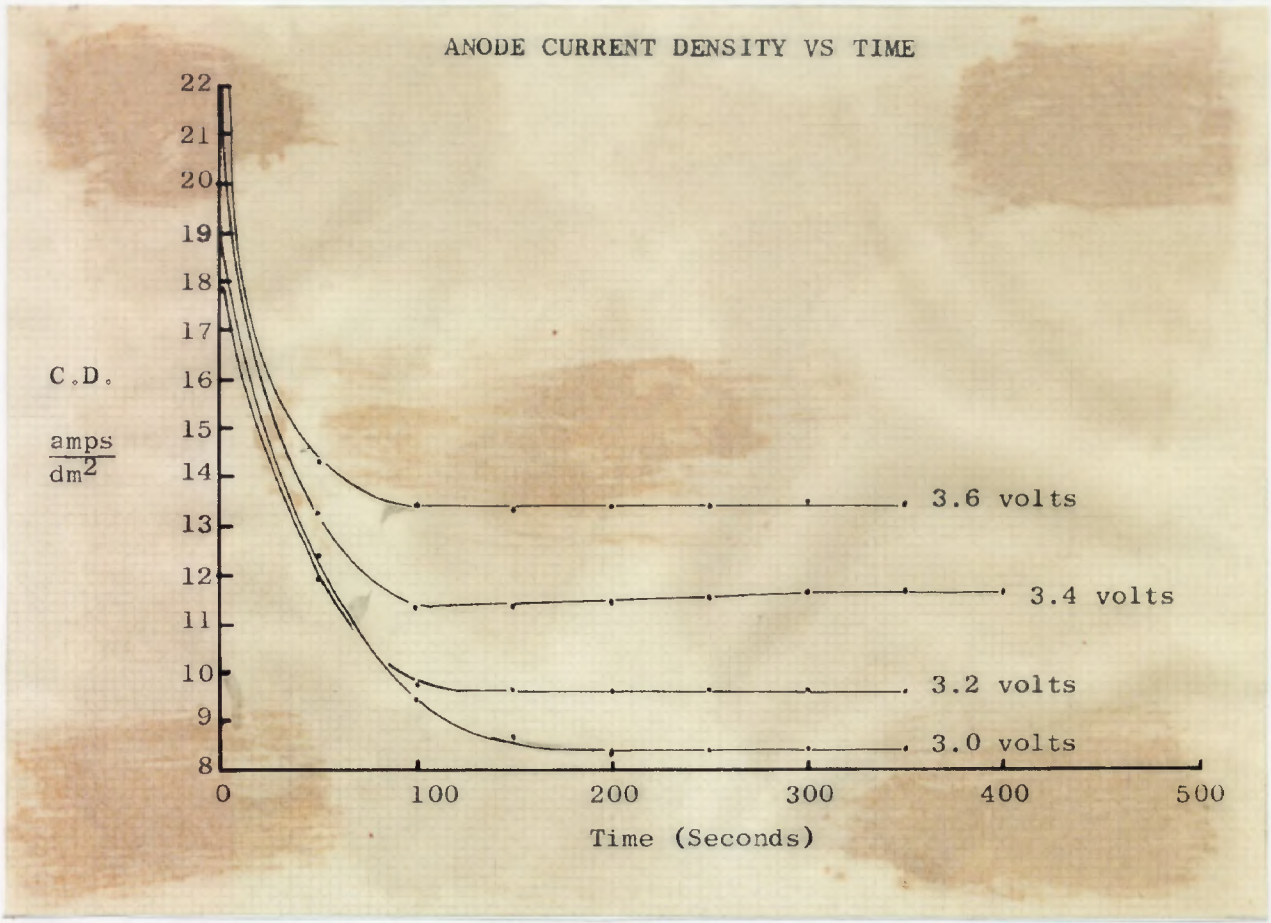

Figure 10. Anode current density vs. time for the polishing plateau.

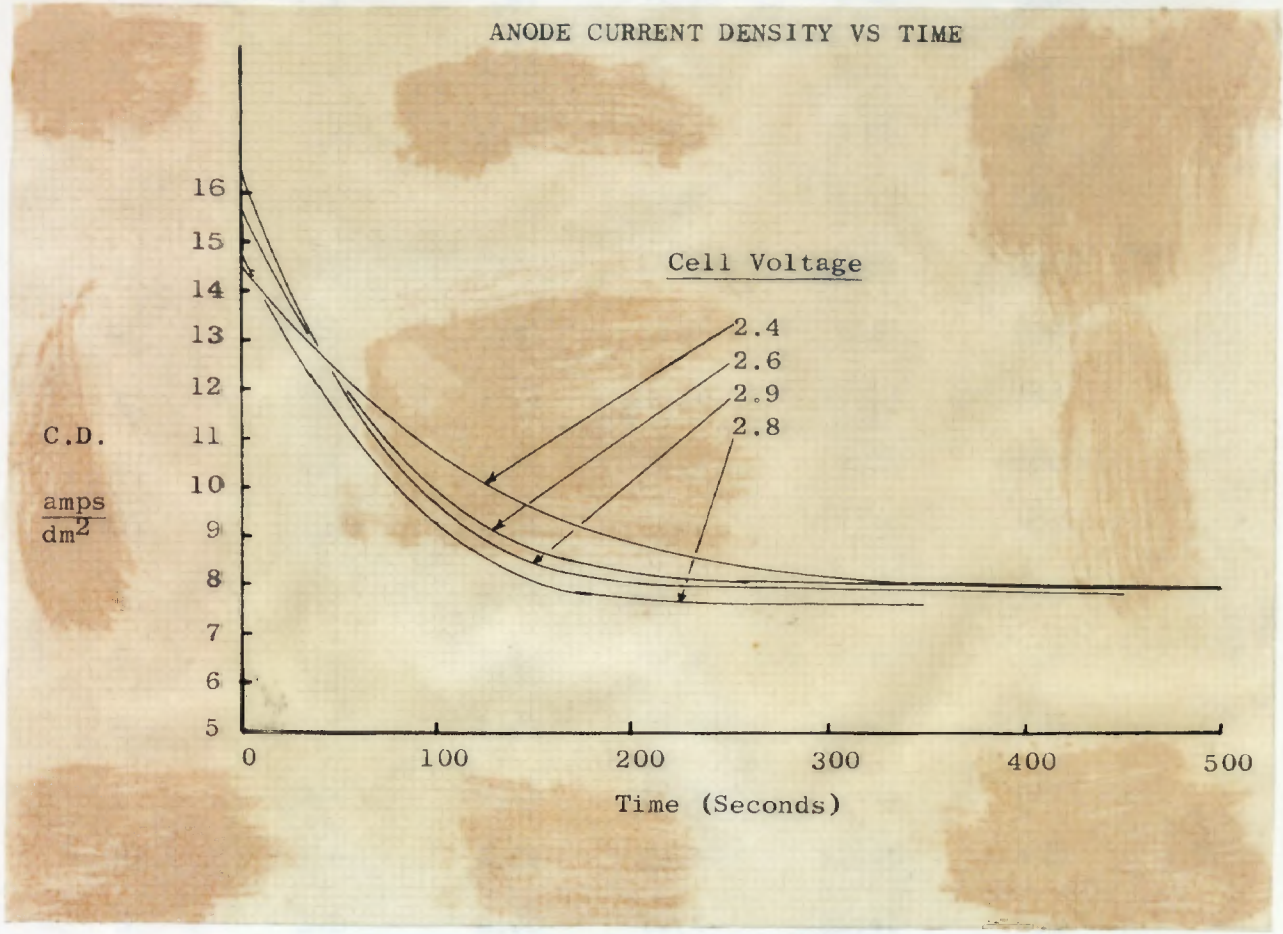

Figure 11. Anode current density vs. time for the slow gas evolution region.

Table I

Sample #	Voltage	Amps Current	Anode area cm^2	C.D. $amps/dm^2$	Time (sec.)
E	1.0	.25	24.95	1.00	600
(F)	1.2	.57	21.5	2.65	600
G	1.4	.83	23.2	3.58	600
H	1.6	1.52	23.2	6.55	600
H'	1.7	1.72	22.8	7.54	600
I	1.8	1.97	22.6	8.72	600
I'	1.9	1.73	22.4	7.73	300
J	2.0	1.83	22.4	8.17	600
K	2.2	1.72	21.9	7.85	600
L	2.4	1.74	22.2	7.85	600
(M)	2.6	1.81	22.8	7.94	600
N	2.8	1.73	22.8	7.58	350
O	2.9	1.78	22.8	7.82	450
P	3.0	1.92	22.8	8.42	400
Q	3.2	2.17	22.5	9.66	350
(R)	3.4	2.68	23.0	11.65	400
S	3.6	3.02	22.4	13.42	350
T	6.0	9.3	22.8	40.8	100
(U)	6.0	9.5	22.8	41.6	350
V	7.8	14.5	22.8	63.7	50

Run III
50% H_3PO_4
1.5" Electrode spacing
Anode to cathode area ratio- 1:1.65

Note: The enclosed ( ) sample numbers were the ones chosen to obtain the four types of surfaces desired according to the experiment. Subsequent analysis dealt with these four samples.

Table II

Sample #	Voltage	Amps Current	Anode area cm^2	C.D. $amps/dm^2$	Time (sec.)
E	1.0	.26	22.6	1.15	600
F	1.2	.65	22.6	2.88	600
G	1.4	1.00	22.6	4.43	600
H	1.6	1.21	22.2	5.45	600
H'	1.7	1.40	22.2	6.32	600
I	1.8	1.48	22.2	6.67	600
I'	1.9	1.55	22.2	6.98	600
J	2.0	1.60	22.2	7.22	600
J'	2.1	1.60	22.2	7.22	600
K	2.2	1.67	22.2	7.53	600
L	2.4	1.55	22.2	6.98	600
M	2.6	1.56	22.0	7.09	600
N	2.8	1.60	22.0	7.28	600
O	3.0	1.80	22.2	8.12	600
P	3.2	2.15	22.2	9.68	350
Q	3.4	2.30	21.7	10.60	350
R	2.3	1.57	22.0	7.15	600
S	2.5	1.56	21.9	7.12	600

Run II
50% H_3PO_4
1.5" Electrode spacing
Anode to cathode area ratio - 1:1.05

B) Electropolishing and Electrodeburring of Nickel Silver

While pursuing the electropolishing of copper investigation, interest was shown by the finishing group (at Western Electric, Kearny Works), in an electropolishing process which would be capable of deburring nickel silver contact springs. Consequently, the same approach as applied to the copper research was performed with nickel silver coupons. The anode current density vs. voltage curve was determined, and each specimen was examined metallographically. By so doing, the appropriate region of the curve where deburring may be accomplished, could be observed. However, before this approach could be pursued, it was necessary to determine the electrolyte best suited for this study.

1) Choice of bath for treating nickel silver. A brief review of the information gathered from a search of the literature, especially the patents of C. L. Faust,[26,27,28] is presented to show how the final bath was established. The basic bath for treating nickel and its alloys is:

	wt.%
H_3PO_4	63
H_2SO_4	15
H_2O	27
Temp.	115 - 130 F

The disadvantage of this bath is that the nickel removed from the anode precipitates as $NiSO_4$ on the heating coils and cathodes causing inefficient polishing, via increased voltage and heating requirements.

The additions of trivalent aluminum and chromium allows the bath to be operated at conditions which decrease the amount of $NiSO_4$ precipitated, thereby requiring less reconditioning of the bath. The addition of chloride (HCl) instead of AL^{+++} and Cr^{+++} causes the undissolved nickel to plate out on the cathode, thus eliminating the $NiSO_4$ precipitation problem. It also enables operation at lower temperature and current density, and although the HCl is not essential for the production of a brilliant mirror-like electropolish, the addition of small percentages of HCl does serve to make possible continuous operation without appreciable precipitation of nickel salts, change in viscosity or increase in tank voltage. Accordingly, .08 wt. % of HCl was added to the basic bath, and a temperature of 100° F was maintained. The polishing plateau was about 3 volts; however, a preferential attack of the nickel was observed, causing pits and the formation of $CuSO_4$ on areas of exposed surface copper. Very short operating times (about 50 seconds) were required to eliminate this condition but did not give the desired results. Consequently, various additions to the basic bath were tried in an effort to eliminate this problem. Since the nickel silver was alloy D, with a composition: 12% Ni, 29% Zn, 59% Cu; H_3PO_4 by itself was tried, since this bath could be used for copper alloys. The H_2SO_4 component in the basic bath was necessary because the H_3PO_4 by itself does not have good throwing power. Since the test coupons were flat, this effect was not noticeable when the 50% orthophosphoric acid bath was used. The results were similar to that

of copper (Figure 12), and in the fast gas evolution region, it was observed that deburring could be accomplished. Section (II-B3) discusses the deburring of nickel silver springs.

2) Electropolishing nickel silver. As mentioned previously, all of the coupons processed were metallurgically examined by a Leitz metallograph. The resulting anode current density vs. voltage curve is analogous to that obtained with copper, and is in accord with the typical curve discussed in section I. The curve is presented in figure 12 and the associated data given in table III. Comparing figure 12 with figure 6, it is seen that the curves are very similar, except for the shorter polishing plateau and shallower unstable region obtained with nickel silver. The analysis of the curve with respect to the four regions, is similar to that presented for copper. The significant difference is that in this case, the anode was an alloy. As a result, the micrographs show areas of preferential attack due to heterogeneous clusters of the alloy constituents.

The required operating conditions to obtain the four types of surfaces on copper and nickel silver are summarized in table IV.

In both cases, a 50% H_3PO_4 solution was used; the electrode spacing was 1.5"; the anode to cathode area ratio was 1:1.65 for copper and 1:1.30 for nickel silver.

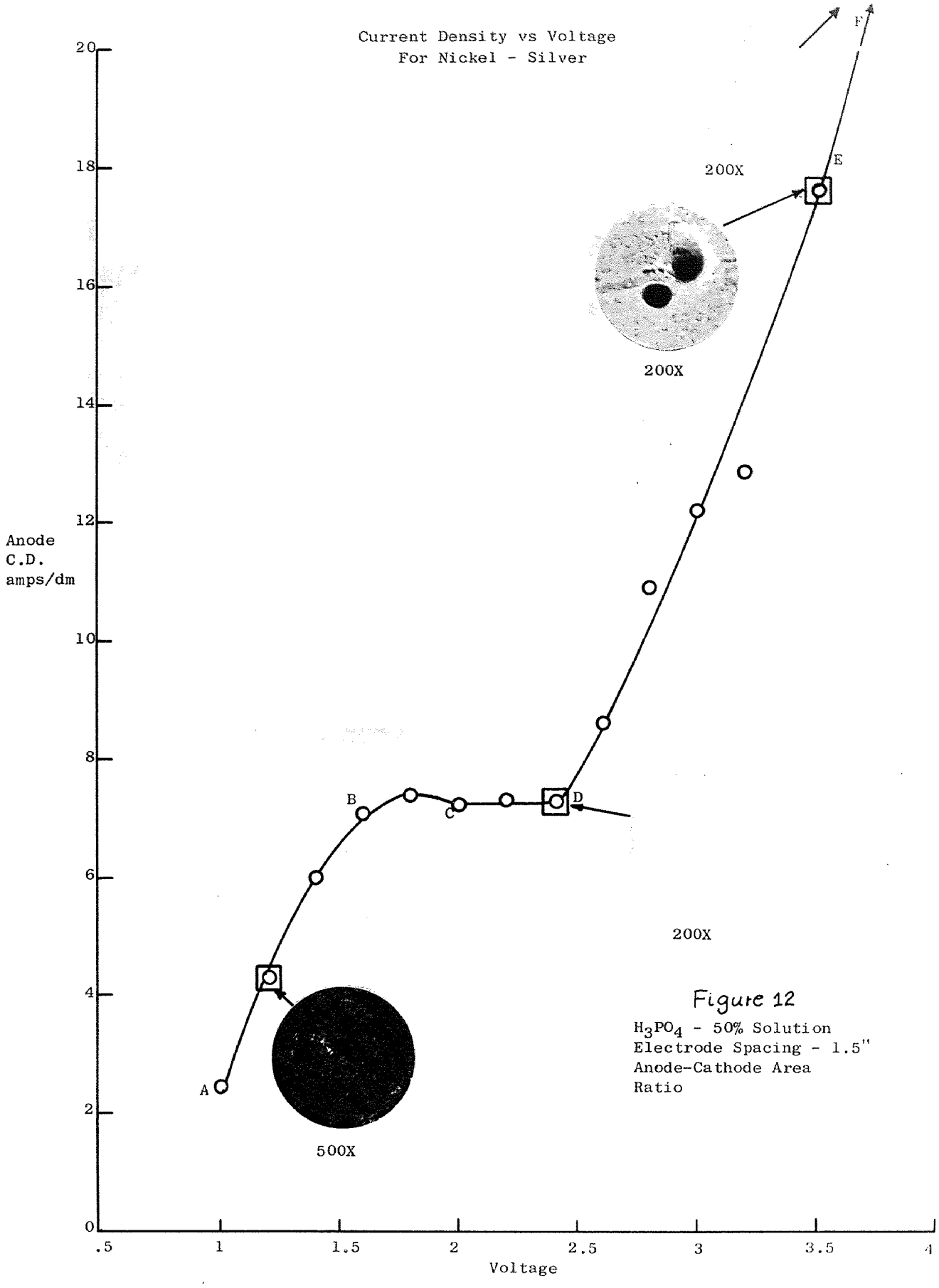

Figure 12

H_3PO_4 - 50% Solution
Electrode Spacing - 1.5"
Anode-Cathode Area
Ratio

Table III

Sample #	Voltage	Amps Current	Anode area cm^2	C.D. $amps/dm^2$	Time (sec.)
A	1.0	.65	26.8	2.42	300
(B)	1.2	1.13	26.8	4.22	300
C	1.4	1.58	26.4	5.98	300
D	1.6	1.90	26.8	7.10	300
E	1.8	1.98	26.8	7.39	300
F	2.0	1.94	26.8	7.24	300
G	2.2	2.00	27.4	7.30	300
(H)	2.4	2.00	27.4	7.30	300
I	2.6	2.32	26.9	8.63	300
J	2.8	3.10	28.4	10.92	300
K	3.0	3.42	28.0	12.22	300
L	3.2	3.75	29.1	12.90	300
(M)	3.5	5.10	28.8	17.70	300
N	4.0	7.20	28.6	25.10	300
P	5.0	10.40	28.1	37.00	100
Q	6.0	15.00	29.1	51.60	300
R	7.0	19.60	29.0	67.70	200
(S)	7.0	18.00	19.4	93.00	200

Run II, Nickel silver
50% H_3PO_4
1.5" Electrode spacing
Anode to cathode area ratio - 1:1.30

COPPER

Surface	Voltage	Current density $\frac{amps}{dm^2}$	Time (sec)
Etched	1.6	6-7	600
Smooth	2.6	7.7-8.2	500
Pitted	3.4	11.5-12.5	300
Smooth and Slightly Pitted	6.0	41-47	300

NICKEL SILVER

Surface	Voltage	Current density $\frac{amps}{dm^2}$	Time (sec)
Etched	1.2	4-5	300
Smooth	2.4	7.1-7.5	300
Pitted	3.4	17-18	300
Smooth and Slightly Pitted	7.0	90-100	200

3) Electrodeburring of nickel silver contact springs. While treating the nickel silver coupons, it was observed that in the fast gas evolution region, the removal of small burrs was achieved. To pursue this further, a batch of nickel silver contact springs, which exhibited the usual burrs from a blanking operation, was obtained from the Kearny Works. The contact spring which is shown in figure 13, is one of a variety of shapes manufactured at Western Electric, Kearny Works. The springs are held with a bayonet placed through one of the holes. They are then degreased, and annealed on the back edge of the spring, to enable a severe forming operation in this area. It is during this annealing operation that the burrs are objectionable. The burrs cause random spaces in the stack, resulting in a non-uniform anneal. As an outgrowth of this study, it has been established that deburring can be accomplished in the fast gas evolution region. The transition from laboratory to shop must be made; if this is possible, by including a deburring step in the manufacturing sequence, this problem can be eliminated. To date, this transition has not been achieved. Figures 14 through 16 show various areas of the specimen before and after deburring. The operating conditions were the same as those given in table IV, except that deburring times of 60 to 100 seconds were sufficient, and the cathode to anode ratio was quite high. Figures 14a and 14b show the region in one of the holes of the spring before and after deburring, at a magnification of 80X. Figures 15a and 15b are the same as those of figure 14, except the magnification was increased to 160X. Figures 16a and 16b show an

edge of the spring before and after deburring, at a magnification of 160X. The surface finish of the springs was similar to that obtained on the coupons.

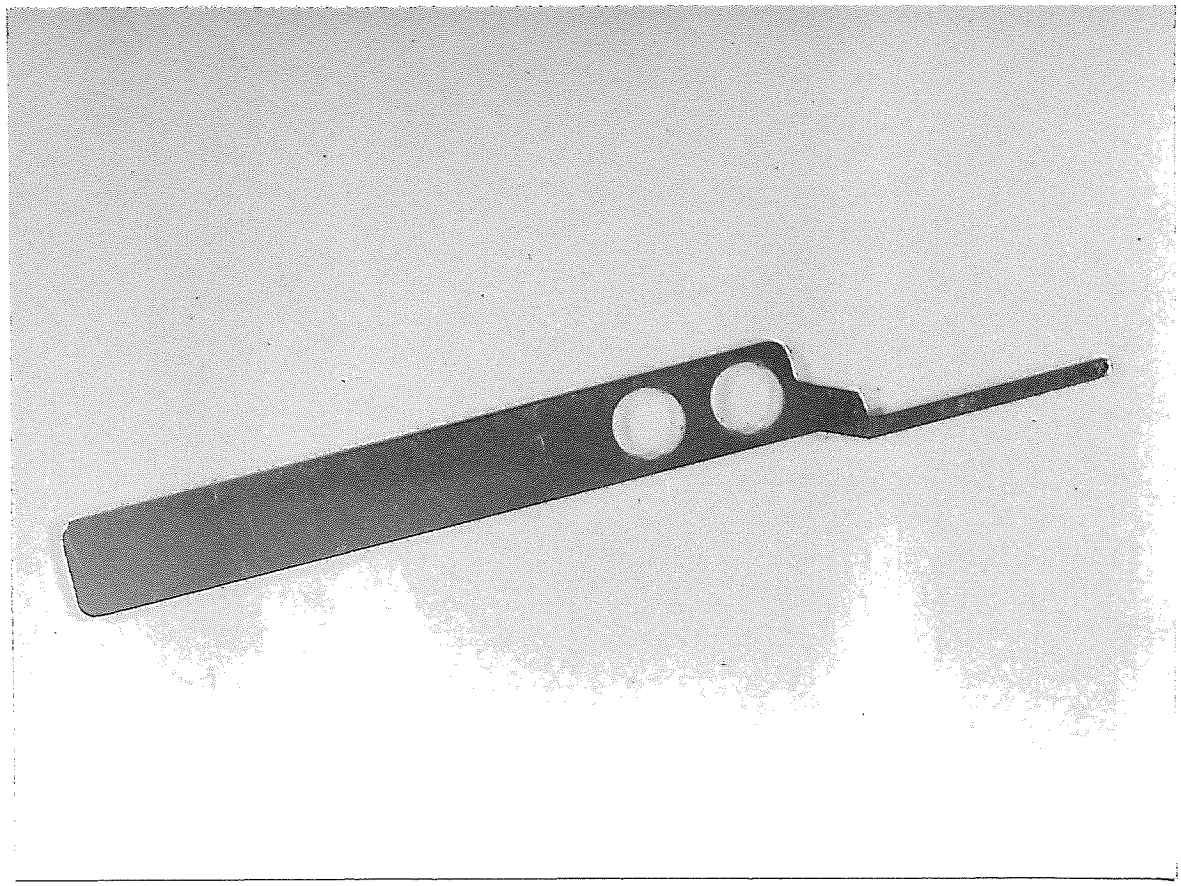

Figure 13. 1.7X, Nickel silver contact spring manufactured at Western Electric, Kearny Works.

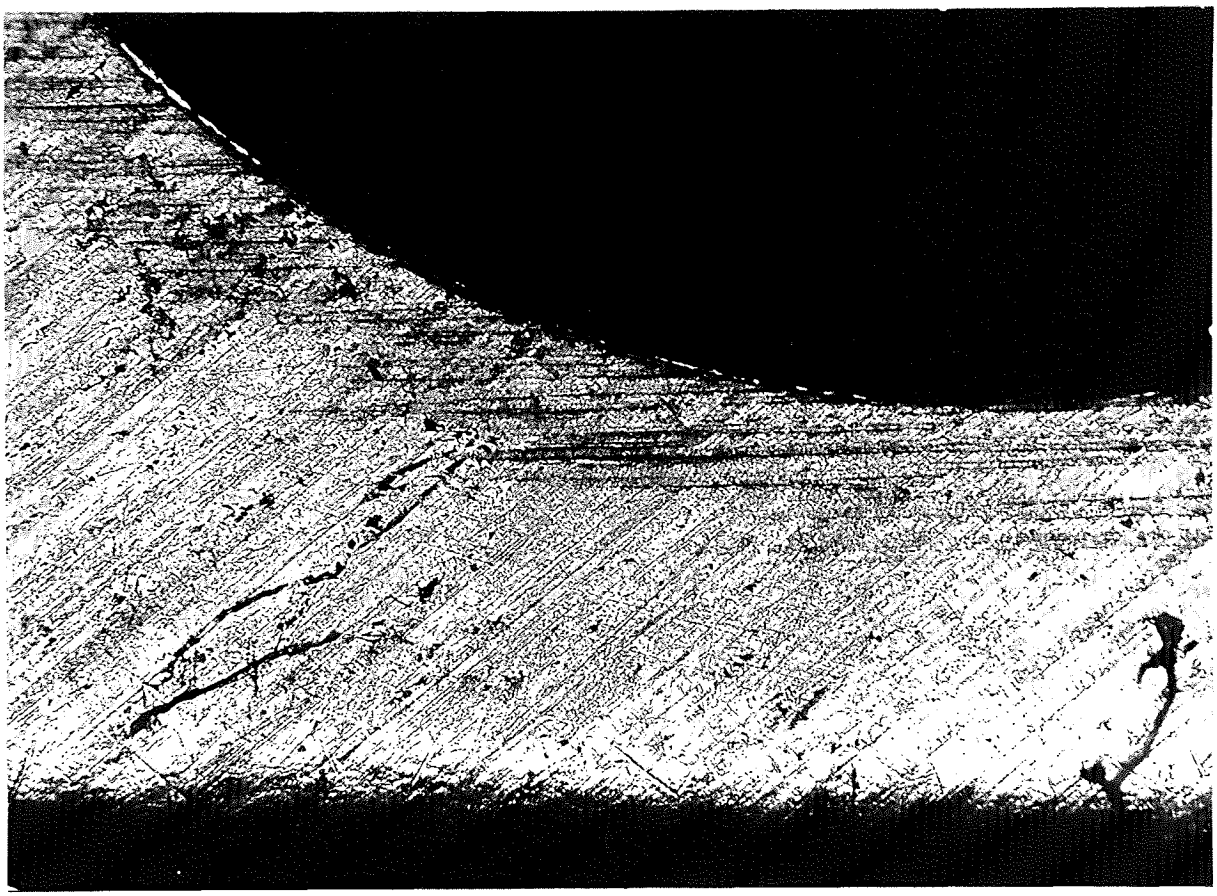

Figure 14a. 80X, Hole region of nickel silver contact spring before deburring.

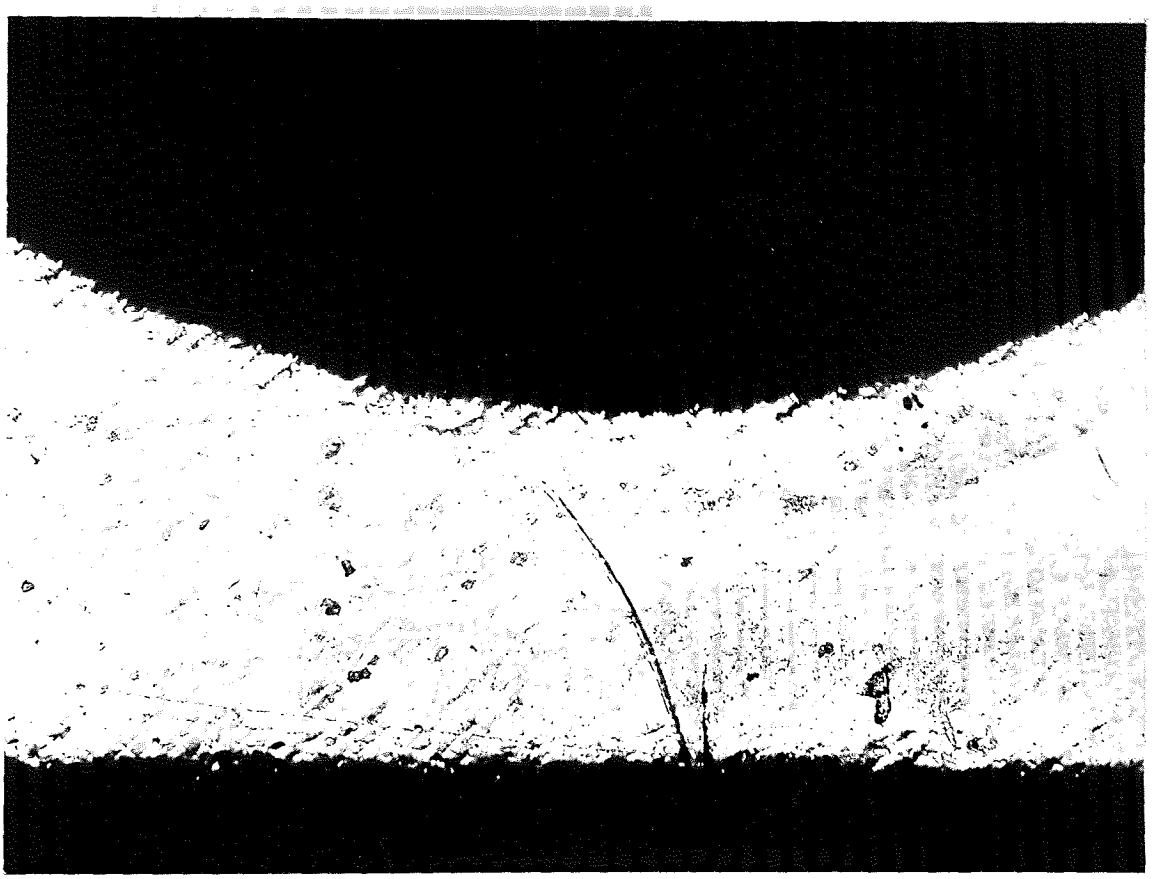

Figure 14b. 80X, Hole region of nickel silver contact spring after deburring.

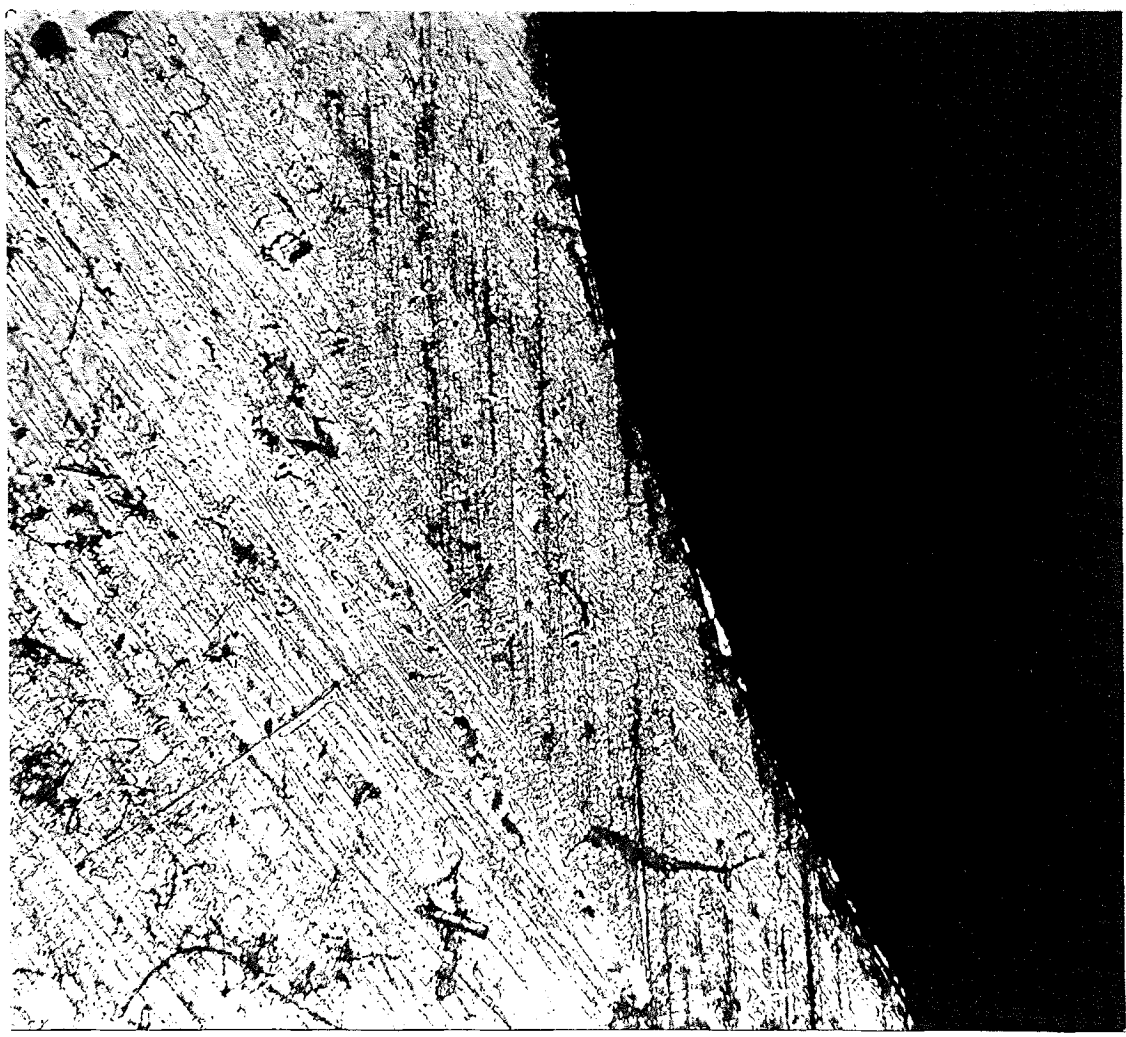

Figure 15a. 160X, Hole region of nickel silver contact spring before deburring.

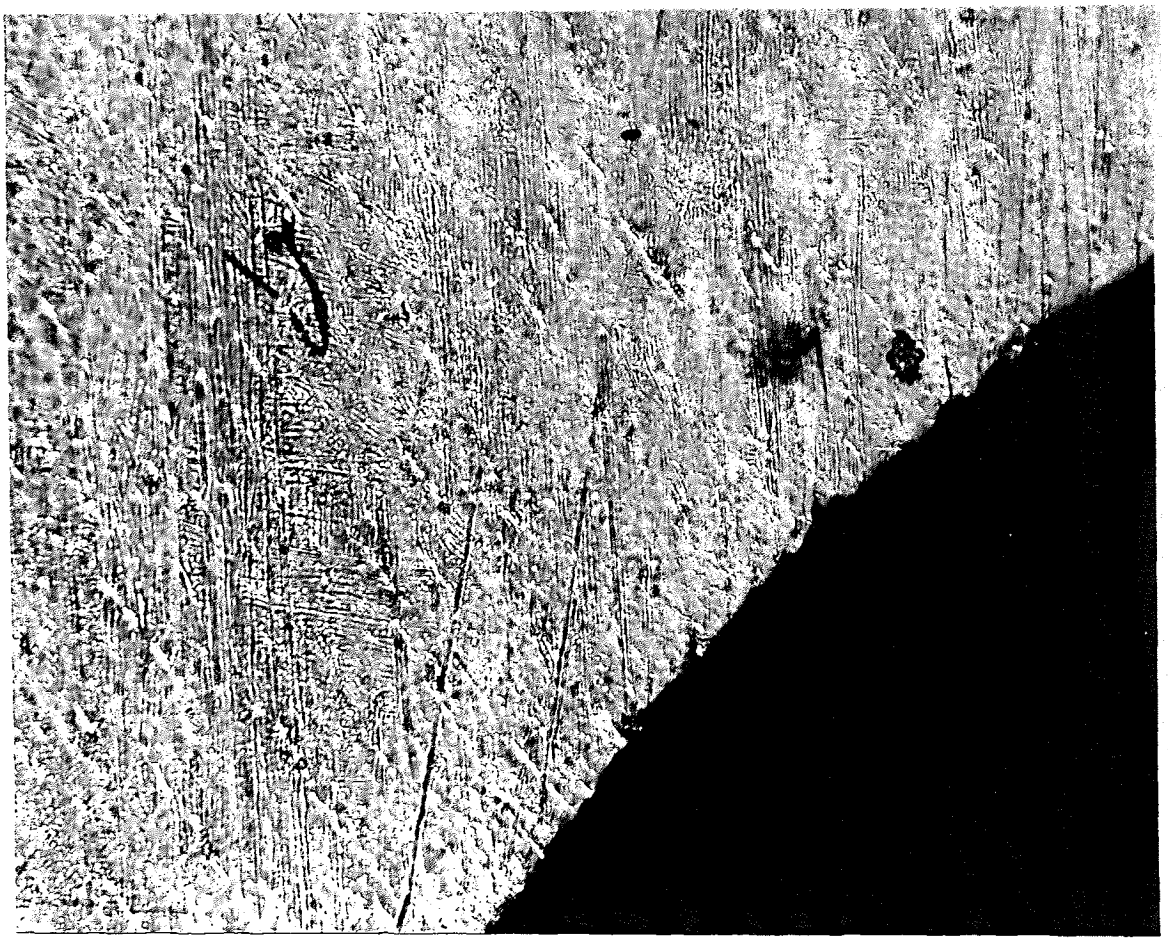

Figure 15b. 160X, Hole region of nickel silver contact spring after deburring.

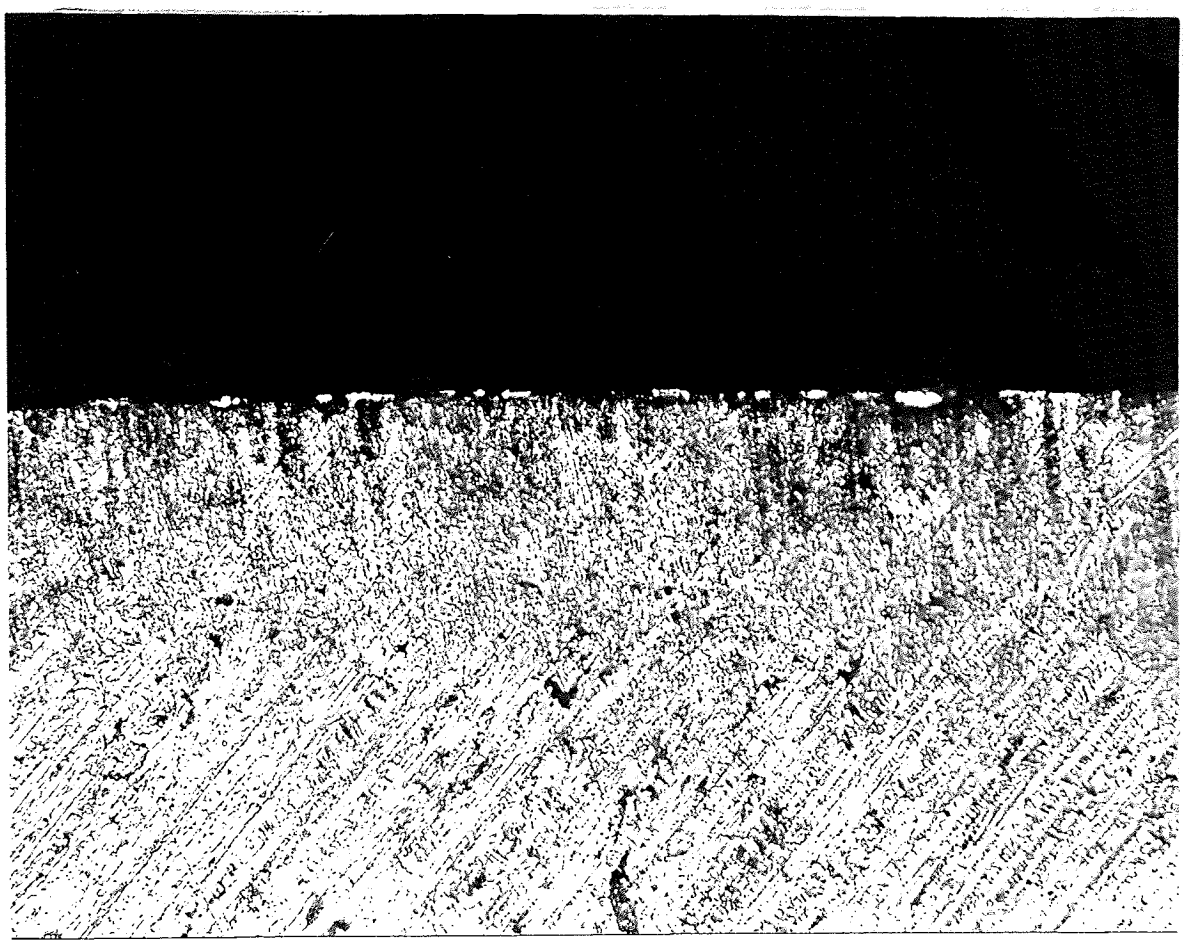

Figure 16a. 160X, Edge region of nickel silver contact spring before deburring.

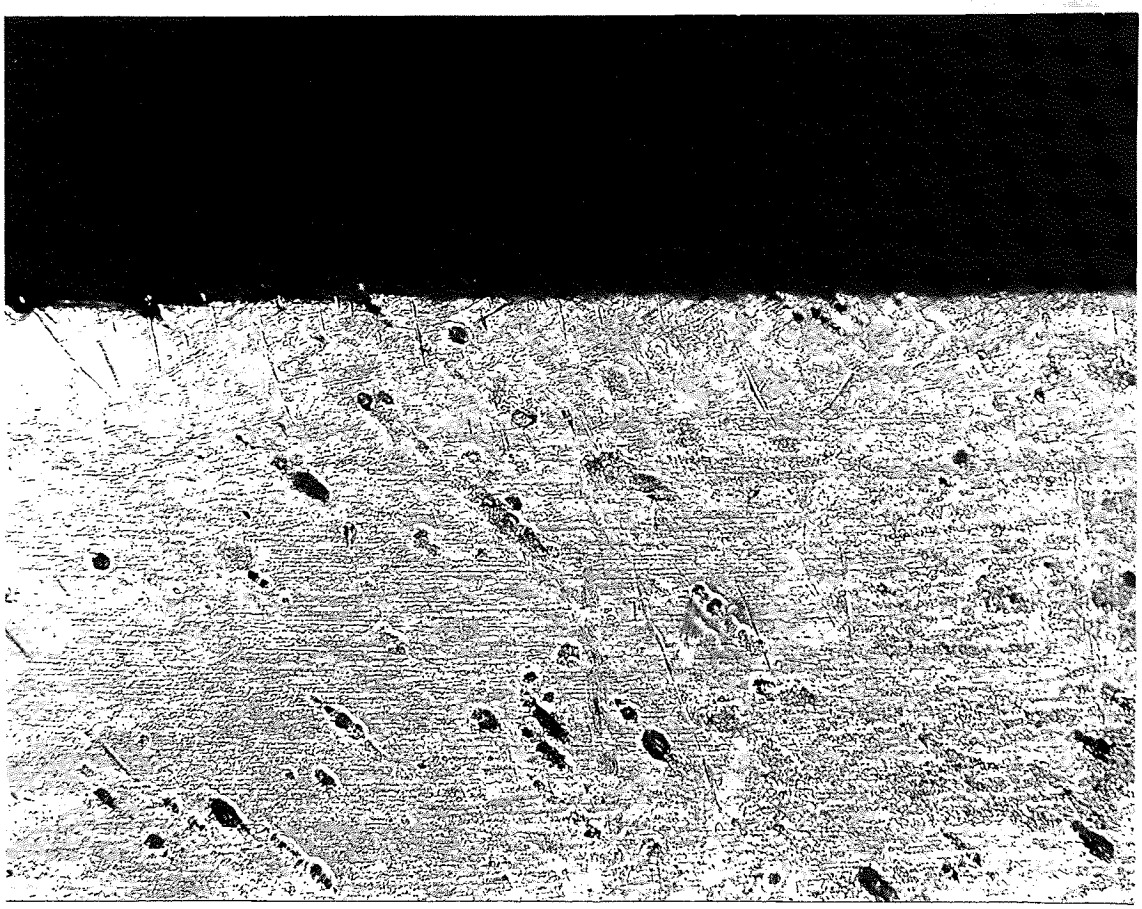

Figure 16b. 160X, Edge region of nickel silver contact spring after deburring.

III STATISTICAL ANALYSIS OF THE DATA

As mentioned previously, the object of this investigation was to obtain various surface finishes to facilitate the study of surface condition on ultrasonic weldability. Electrolytic polishing was used to obtain the desired surface finishes, and as indicated by the data and micrographs presented in section II, four types of surfaces were obtained. For a given set of parameters, if the anode current density vs. voltage curve is plotted, one observes that there are four regions of this curve which correspond to the four types of surface finishes obtained. A typical curve as predicted by the current theory is shown in figure 6. Since this curve appear to be composed of three distinct curves, the curve obtained experimentally was separated into three portions and a regression analysis using the method of least squares was employed to get the "best-fit" for the data obtained. The details of this statistical analysis for the etching region, polishing plateau and gas evolution region comprise the first segment of section III. Briefly it was found that in the etching region, a complex polynomial model is required to fit the curve and explain the blip (unstable region) predicted by current electropolishing theory. On the polishing plateau the simple model $y = \bar{y}$ was the best fit model. In the gas evolution region a quadratic regression model gave the best fit.

The second half of this section is devoted to a statistical analysis of the data resulting from the Talysurf profilometer traces.

Consistent with the primary object of the experiment, the intent of the statistical analysis was to determine if each of the four surfaces obtained were significantly different from each other. That is, does four different populations exist? Utilizing the look test, $\bar{X}$ and R Chart, t test between samples F and U, and the runs test where ties could be handled; it was found that four different populations did exist.

A) Regression analysis

A regression analysis was applied to the curve in figure 6, which was plotted from the data in table I.

Table I

Sample #	Voltage	Amps Current	Anode area cm^2	C.D. $amps/dm^2$	Time (sec.)
E	1.0	.25	24.95	1.00	600
(F)	1.2	.57	21.5	2.65	600
G	1.4	.83	23.2	3.58	600
H	1.6	1.52	23.2	6.55	600
H'	1.7	1.72	22.8	7.54	600
I	1.8	1.97	22.6	8.72	600
I'	1.9	1.73	22.4	7.73	300
J	2.0	1.83	22.4	8.17	600
K	2.2	1.72	21.9	7.85	600
L	2.4	1.74	22.2	7.85	600
(M)	2.6	1.81	22.8	7.94	600
N	2.8	1.73	22.8	7.58	350
O	2.9	1.78	22.8	7.82	450
P	3.0	1.92	22.8	8.42	400
Q	3.2	2.17	22.5	9.66	350
(R)	3.4	2.68	23.0	11.65	400
S	3.6	3.02	22.4	13.42	350
T	6.0	9.3	22.8	40.8	100
(U)	6.0	9.5	22.8	41.6	350
V	7.8	14.5	22.8	63.7	50

Run III
50% H_3PO_4
1.5" Electrode spacing
Anode to cathode area ratio- 1:1.65

Note: The enclosed ( ) sample numbers were the ones chosen to obtain the four types of surfaces desired according to the experiment. Subsequent analysis dealt with these four samples.

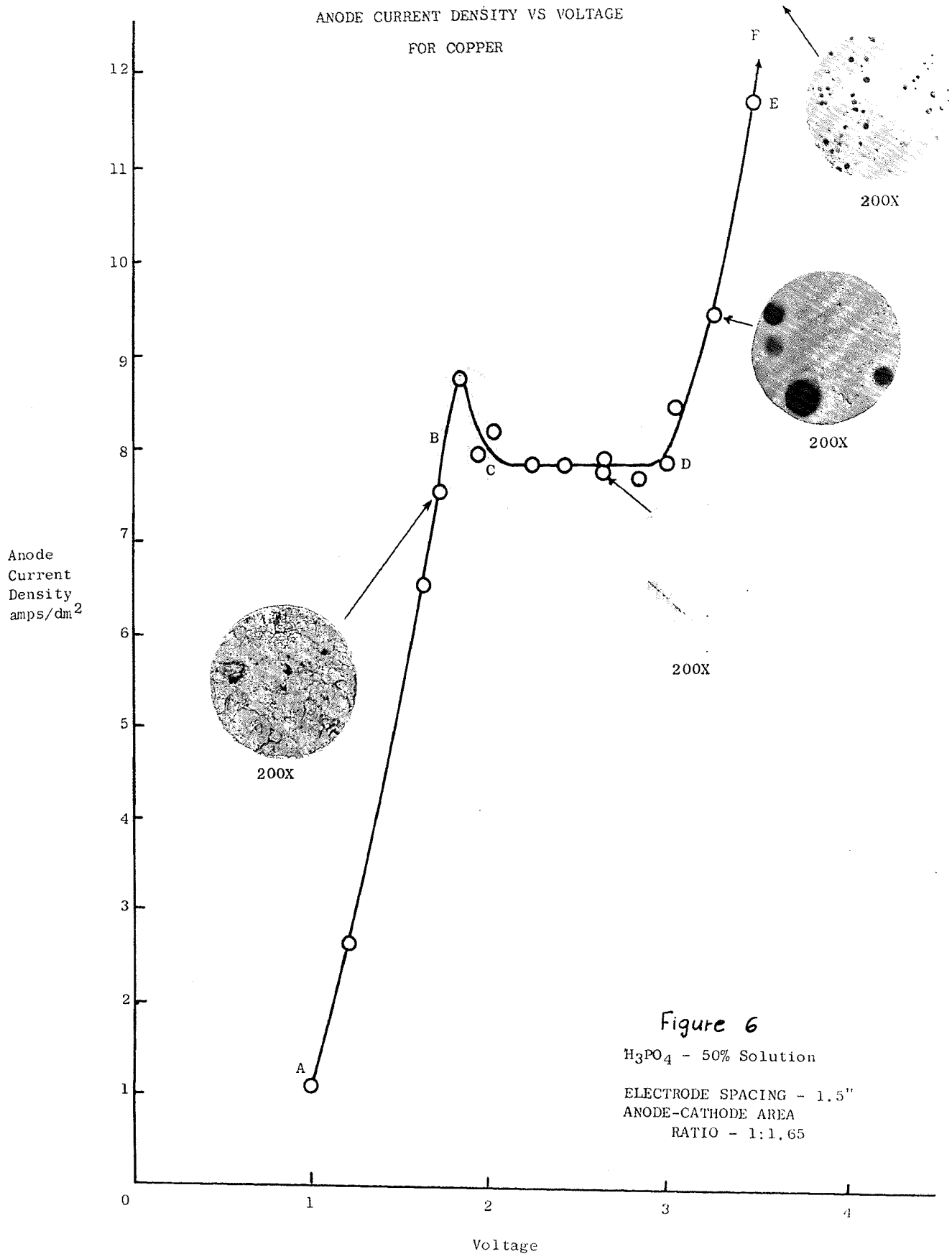

Figure 6

H_3PO_4 - 50% Solution

ELECTRODE SPACING - 1.5"
ANODE-CATHODE AREA
RATIO - 1:1.65

Etching Region of Curve - Linear Regression Model

y	x	xy	x^2	x^2y	x^4	x^3
1.00	1.0	1.00	1.00	1.00	1.00	1.00
2.65	1.2	3.18	1.44	3.82	2.07	1.73
3.58	1.4	5.02	1.96	7.02	3.84	2.74
6.55	1.6	10.48	2.56	16.77	6.55	4.10
7.54	1.7	12.80	2.89	21.79	8.35	4.91
8.72	1.8	15.68	3.24	28.25	10.50	5.83
7.73	1.9	14.70	3.61	27.91	13.03	6.86
8.17	2.0	16.34	4.00	32.68	16.00	8.00
Σ 45.94	12.6	79.20	20.70	139.24	61.34	35.17

$\bar{y} = 5.74$ $\bar{x} = 1.57$

$y = a + bx$

Find values for a and b which make the sum of squares a minimum.

$\Sigma y = na + b\Sigma x$ $45.94 = (8)a + (12.6)b$

$\Sigma yx = a\ x + b\Sigma x^2$ $79.20 = (12.6)a + (20.7)b$

Solving these equations:

$a = -6.867$

$b = 8.006$

check, $\bar{y} = 5.74$, $\bar{x} = 1.57$

$\bar{y} = -6.867 + 8.006(1.57)$

$= 5.70$

Thus, $y = -6.867 + 8.006x$

x	y_o	y_c	$(y_o - y_c)$	$(y_o - y_c)^2$
1.0	1.00	1.14	.14	.0196
1.2	2.65	2.93	.29	.0841
1.4	3.58	4.34	.76	.5776
1.6	6.55	5.94	.61	.3758
1.7	7.54	6.74	.80	.6400
1.8	8.72	7.54	1.18	1.3830
1.9	7.73	8.34	.61	.3770
2.0	8.17	9.15	.98	.9506
				4.4077

For $y = \bar{y} = 5.74$ $\quad (y-\bar{y})^2 = (4.74)^2 + (3.09)^2 + (2.16)^2 + (.81)^2 + (1.80)^2 + (2.98)^2 + (1.99)^2 + (2.43)^2$

$= 59.30$

Therefore;

$y = \bar{y}$; $\quad (y-\bar{y})^2 = 59.30$ $\quad$ degrees of freedom (d.f.) = 7

$y = a + bx$ $\quad (y + 6.87 - 8.0x)^2 = 4.408$ $\quad$ d.f. = 6

Source of variation	Sum of squares	d.f.	Mean sq.	F
Slope	54.892	1	54.892	74.7
Error	4.408	6	0.735	
Total	59.30	7		

$F_{.05/1/6} = 6.0$

Thus, this model is a "good fit", but it does not account for the blip observed in this region. This blip, known as the unstable region, is in accordance with the current theory. Therefore, a quadratic model will be tried next.

Parabola Model: $y = a + bx^2$

Find values of a and b which make the sum of squares a minimum.

$\sum y = na + b\sum x^2$

$\sum x^2y = a\sum x^2 + b\sum x^4$

Substituting the data from page 60 gives:

$45.94 = (8)a + (20.70)b$

$139.24 = (20.7)a + (61.34)b$

Solving these equations gives:

$a = -1.034$

$b = 2.619$

Thus, $y = -1.034 + 2.619x^2$

x	y_o	y_c	$(y_o - y_c)$	$(y_o - y_c)^2$
1.0	1.00	1.585	.585	.3422
1.2	2.65	2.737	.087	.0076
1.4	3.58	4.099	.519	.2694
1.6	6.55	5.671	.879	.7726
1.7	7.54	6.535	1.005	1.0100
1.8	8.72	7.452	1.268	1.6078
1.9	7.73	8.421	.691	.4775
2.0	8.17	9.442	1.272	1.6180
				6.1954

The sum of squares for this model (error about regression for the parabola) calculates to be greater than the sum of squares for the linear model $y = a + bx$, (see the bottom of page 60). Therefore, this parabola model is not as good a fit as the linear model.

It should be mentioned that this result, although not common, is explainable by closely analyzing the data in the etching region of the curve. Below is a sketch showing the observed data, the $y = a + bx$ model and the $y = a + bx^2$ model. By checking $(y_o - y_c)$ for each model, it is observed that the values close to the blip are causing the discrepancy. By going to this model, we did not sacrifice another degree of freedom, i.e. both models "cost" two degrees of freedom, thus the linear model is a better fit.

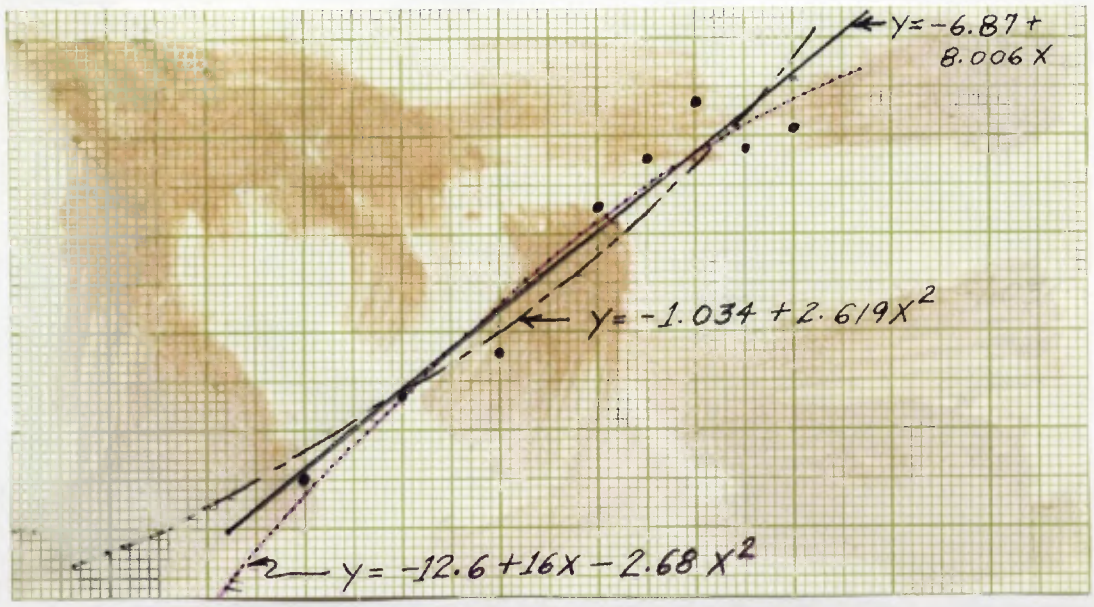

A third model for this region, $y = a + bx + cx^2$ will be tried next in an attempt to get a better fit, especially near the blip.

Polynomial Model: $y = a + bx + cx^2$

Find values for a, b and c which make the sum of squares a minimum.

$$\Sigma y = na + b\Sigma x + c\Sigma x^2$$

$$\Sigma xy = a\Sigma x + b\Sigma x^2 + c\Sigma x^3$$

$$\Sigma x^2y = a\Sigma x^2 + b\Sigma x^3 + c\Sigma x^4$$

Substituting the data from page 60 gives:

$$45.94 = (8)a + (12.6)b + (20.7)c$$

$$79.20 = (12.6)a + (20.7)b + (35.17)c$$

$$139.24 = (20.7)a + (35.17)b + (61.34)c$$

Solving these equations by determinants (see page 65) gives:

$$a = -12.6$$

$$b = 16.0$$

$$c = -2.68$$

Thus, $y = -12.6 + 16.0x - 2.68x^2$ It is interesting to note that this model, which is a better fit than the parabola model, curves the other way. (see sketch on previous page)

x	y_o	y_c	$(y_o - y_c)$	$(y_o - y_c)^2$
1.0	1.00	.72	.28	.0784
1.2	2.65	2.74	.09	.0081
1.4	3.58	4.55	.97	.9409
1.6	6.55	6.14	.41	.1681
1.7	7.54	6.90	.64	.4096
1.8	8.72	7.52	1.20	1.4400
1.9	7.73	8.12	.39	.1521
2.0	8.17	8.68	.51	.2601
				3.4573

Therefore:

Model	$y = \bar{y}$	$(y-\bar{y})^2 = 59.3$	d.f. = 7
Model	$y = a + bx$	$(y + 6.87 - 8.0x)^2 = 4.408$	d.f. = 6
Model	$y = a + bx + cx^2$	$(y+12.6- 16x+2.68x^2)^2 = 3.457$	d.f. = 5

Source of variation	Sum of squares	d.f.	Mean sq.	F
Quadratic	0.951	1	.951	1.376
Error	3.457	5	.691	
Total	4.408	6		

$$F_{.05/1/5} = 6.6$$

Thus, this model which gives the least sum of squares (error about regression for quadratic), could have been obtained by "chance", since by sacrificing a degree of freedom, we only reduced the error sum of squares by 0.951 as compared to the linear model.

Conclusion: In this region of the curve, a complex polynomial model is required to fit the curve and explain the blip predicted by the current electropolishing theory. This is beyond the scope of this project so the analysis of this region will be left incomplete. In the remaining two regions, the polishing plateau and the gas evolution region, it is easier to fit a regression model.

Determinant solution for the polynomial model, $Y = a + bX + cX^2$.

$$\Delta = \begin{vmatrix} 8.0 & 12.6 & 20.7 \\ 12.6 & 20.7 & 35.17 \\ 20.7 & 35.17 & 61.34 \end{vmatrix} = 0.47$$

$$a = \frac{\begin{vmatrix} 45.94 & 12.6 & 20.7 \\ 79.20 & 20.7 & 35.17 \\ 139.24 & 35.17 & 61.34 \end{vmatrix}}{\Delta} = \frac{-5.92}{0.47} = -12.6$$

$$b = \frac{\begin{vmatrix} 8.0 & 45.94 & 20.7 \\ 12.6 & 79.20 & 35.17 \\ 20.7 & 139.24 & 61.34 \end{vmatrix}}{\Delta} = \frac{7.52}{0.47} = 16.0$$

$$c = \frac{\begin{vmatrix} 8.0 & 12.6 & 45.94 \\ 12.6 & 20.7 & 79.20 \\ 20.7 & 35.17 & 139.24 \end{vmatrix}}{\Delta} = \frac{-1.26}{0.47} = -2.68$$

Polishing Plateau Portion of Curve - $y = \bar{y}$ Model:

x	y
2.2	7.85
2.4	7.85
2.6	7.94
2.8	7.58
2.9	7.82
12.9	39.04
$\bar{x}$ =2.58	$\bar{y}$ = 7.81

Arbitrary model; $y = 0$

$$\sum_{i=1}^{5} (y_i - 0)^2 = 2(7.85)^2 + (7.94)^2 + (7.58)^2 + (7.82)^2 = 304.9$$

degrees of freedom (d.f.) = 5

Best fit model of form $y = \bar{y} = 7.81$

$$\sum_{i=1}^{5} (y_i - \bar{y})^2 = \sum_{i=1}^{5} (y_i - 0)^2 - \sum (\bar{y} - 0)^2$$

$$= 304.9 - 5(7.81)^2 = 0.2 \qquad \text{d.f.} = 4$$

Thus by giving up 1 degree of freedom the sum of squares has been reduced significantly.

Source of variation	Sum of squares	d.f.	Mean sq.	F
$y = \bar{y}$	304.7	1	304.7	very large
Error	0.2	4	0.05	
Total	304.9	5		

Thus $y = \bar{y}$ is the best fit model (see figure 6).

Gas Evolution Region of Curve - Linear Regression Model:

x	y	xy	x^2	x^3	x^2y	x^4
2.9	7.82	22.68	8.41	24.39	65.77	70.73
3.0	8.42	25.26	9.00	27.00	75.78	81.00
3.2	9.66	30.91	10.24	32.77	98.92	104.86
3.4	11.65	39.61	11.56	39.30	134.67	133.63
3.6	13.42	48.31	12.96	46.66	173.92	167.96
6.0	41.20	247.20	36.00	216.00	1483.20	1296.00
7.8	63.7	496.86	60.84	474.55	3875.51	3701.50
29.9	155.87	910.83	149.01	860.67	5907.77	5555.68

$\bar{x} = 4.27$ $\bar{y} = 22.27$

$y = a + bx$

Find values for a and b which make the sum of squares a minimum.

$\sum y = na + b\sum x$ $155.87 = (7)a + (29.9)b$

$\sum xy = a\sum x + b\sum x^2$ $910.83 = (29.9)a + (149.01)b$

Solving these equations gives:

$a = -26.88$

$b = 11.51$

check, should go through $\bar{y}, \bar{x}$

$y = -26.88 + 11.51(4.27)$

$y = 22.24$; $\bar{y}, = 22.27$

Thus, $y = -26.88 + 11.51x$

x	y_o	y_c	$(y_o - y_c)$	$(y_o - y_c)^2$
2.9	7.82	6.50	1.32	1.742
3.2	9.66	9.95	0.29	0.841
3.0	8.42	7.65	0.77	0.593
3.4	11.65	12.25	0.60	0.360
3.6	13.42	14.56	1.14	1.300
6.0	41.20	42.18	0.98	0.960
7.8	63.70	62.90	0.80	0.640
				6.436

For $y = \bar{y} = 22.27$ $\quad (y-\bar{y})^2 = (14.45)^2 + (13.85)^2 + (12.61)^2 +$

$(10.62)^2 + (8.85)^2 + (18.92)^2 + (41.43)^2$

$= 2825.51$

Therefore;

$y = \bar{y}$	$(y-\bar{y})^2 = 2825.51$	d.f. = 6
$y = a + bx$	$(y+ 26.88 - 11.51x)^2 = 6.436$	d.f. = 5

Source of variation	Sum of squares	d.f.	Mean sq.	F
Slope	2819.07	1	2819.07	very big
Error	6.44	5	1.29	
Total	2825.51	6		

$F_{.05/1/5} = 6.6$

Thus, the model $y = - 55.56 + 18.22x$ is a good fit. However, there is still some error (sum of squares = 6.44) associated with this model; therefore a quadratic model will be tried.

Quadratic Model: $y = a + bx + cx^2$

Find the values of a, b and c which make the sum of squares a minmum.

$\sum y = na + b\sum x + c\sum x^2$

$\sum xy = a\sum x + b\sum x^2 + c\sum x^3$

$\sum x^2y = a\sum x^2 + b\sum x^3 + c\sum x^4$

Substituting these values from page 67 gives:

$155.87 = (7)a + (29.9)b + (149.01)c$

$910.83 = (29.9)a + (149.01)b + (860.67)c$

$5907.77 = (149.01)a + (860.67)b + (5555.68)c$

Solving these equations gives; (see page 71 for the determinant solution).

$a = - 16.84$
$b = 7.05$
$c = 0.424$

Thus, $y = -16.84 + 7.05x + 0.424x^2$

x	y_o	y_c	$(y_o - y_c)$	$(y_o - y_c)^2$
2.9	7.82	7.18	.64	.410
3.0	8.42	8.13	.29	.084
3.2	9.66	10.06	.40	.160
3.4	11.65	12.03	.38	.144
3.6	13.42	14.04	.62	.384
7.8	63.70	63.95	.25	.063
6.0	41.20	40.72	.48	.230
				1.475

Therefore:

Model $y = \bar{y}$ $\quad (y-\bar{y})^2 = 2825.51$ $\quad$ d.f. = 6

Model $y = a+bx$ $\quad (y+26.88-11.51x)^2 = 6.436$ $\quad$ d.f. = 5

Model $y = a+bx+cx^2$ $\quad (y+16.84-7.05x-.424x^2)^2 = 1.475$ $\quad$ d.f. = 4

Source of variation	Sum of squares	d.f.	Mean sq.	F
Quadratic	4.961	1	4.961	13.4
Error	1.475	4	.369	
Total	6.436	5		

$$F_{.05/1/4} = 7.7$$

Thus, the model $y = -16.84 + 7.05x + 0.424x^2$ is an excellent fit. This quadratic equation is in support of the theory, and is typical of the gas evolution region. To indicate how good a fit was obtained, a sketch showing the gas evolution region is presented on the following page. The observed points are shown as ⊙. The dotted line is the linear regression model and the full line is the quadratic regression model.

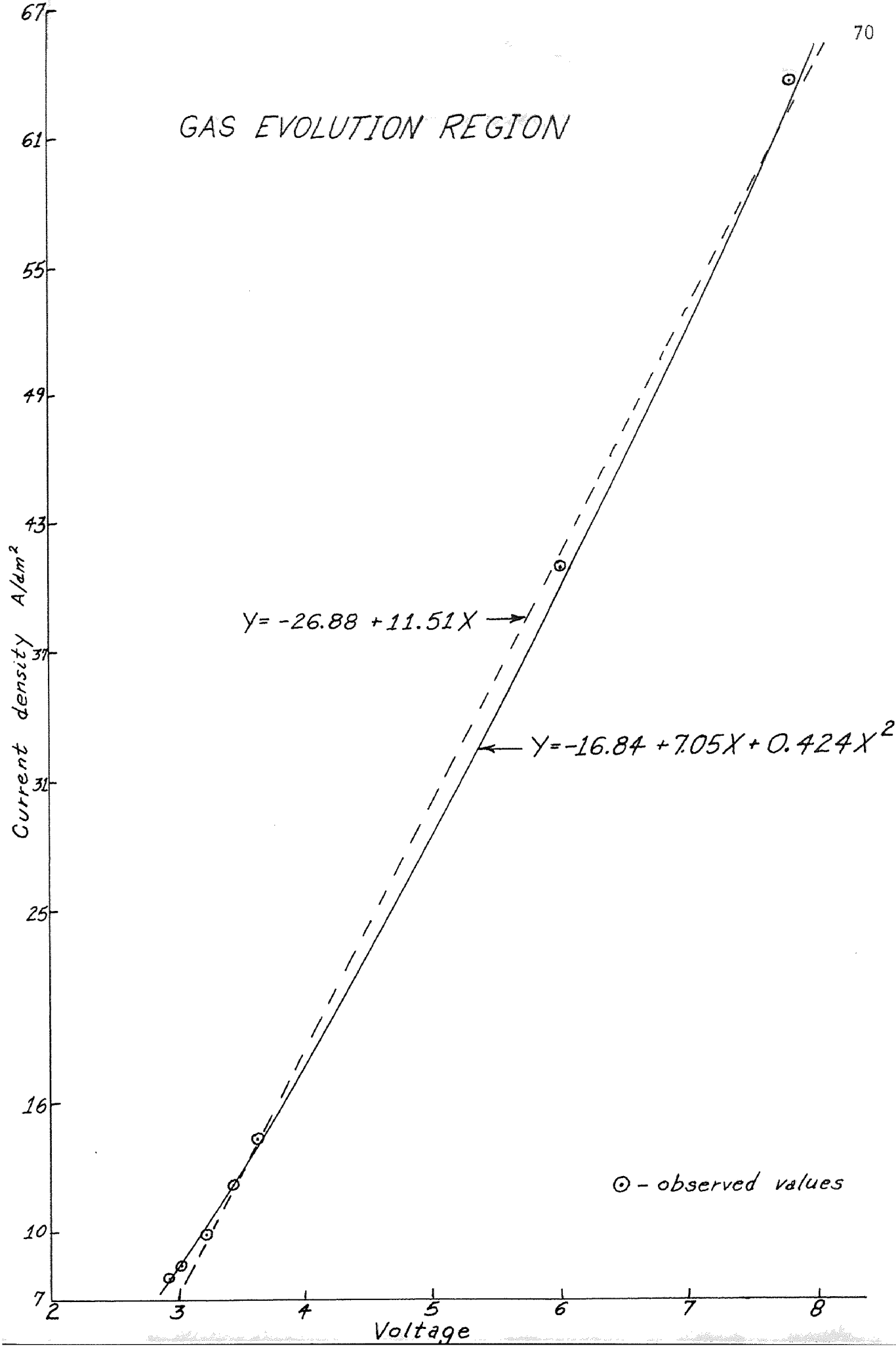
GAS EVOLUTION REGION
Y= -26.88 + 11.51X
Y=-16.84 + 7.05X + 0.424X²
⊙ - observed values
Current density A/dm²
Voltage
67
61
55
49
43
37
31
25
16
10
7
2
3
4
5
6
7
8

Determinant solution for the quadratic model, $Y = a + bX + cX^2$.

$$\Delta = \begin{vmatrix} 7.0 & 29.9 & 149.01 \\ 29.9 & 149.01 & 860.67 \\ 149.01 & 860.67 & 5555.68 \end{vmatrix} = 3500.28$$

$$a = \frac{\begin{vmatrix} 155.87 & 29.9 & 149.01 \\ 910.83 & 149.01 & 860.67 \\ 5907.77 & 860.67 & 5555.68 \end{vmatrix}}{\Delta} = \frac{-58959.53}{3500.28} = -16.84_4$$

$$b = \frac{\begin{vmatrix} 7.0 & 155.87 & 149.01 \\ 29.9 & 910.83 & 860.67 \\ 149.01 & 5907.77 & 5555.68 \end{vmatrix}}{\Delta} = \frac{24663.63}{3500.28} = 7.04_6$$

$$c = \frac{\begin{vmatrix} 7.0 & 29.9 & 155.87 \\ 29.9 & 149.01 & 910.83 \\ 149.01 & 860.67 & 5907.77 \end{vmatrix}}{\Delta} = \frac{1484.28}{3500.28} = 0.424$$

B) Statistical Analysis of Talysurf Data.

Four samples were chosen, one from each region on the curve, which gave the desired surface finish. These samples were examined metallographically at magnifications of 200x to 500x. These micrographs showed quite convincingly that the surfaces were different and were in accord with the regions from which they were treated. However, because of the very small surface area that can be examined this way, and the lack of quantitative data to support the results, another test was sought. The one chosen was measuring the peak to valley distances (surface profile) using a Talysurf Tester. Typical Talysurf traces for the four types of surfaces were presented on pages 34 and 35. The object of the statistical analysis was to determine if each surface was different from the other (i. e. , 4 different populations exist).

Table V

Summary of Talysurf Data - for selected samples of Run III

Sample	Range in Å	$\bar{X}$	S	n
III F	4,000 → 36,000	13,200	7,320	51
III M_a	250 → 2,500	1,100		19
III M_b	300 → 3,500	1,600		16
III M_c	250 → 3,000	1,300	710	19
III M_d	250 → 2,500	1,100		18
		$\bar{\bar{X}}$=1,275		72
III R_a	15,000 → 80,000	39,000		29
III R_b	10,000 → 90,000	36,000	23,800	17
III R_c	10,000 → 70,000	35,000		15
III R_d	10,000 → 80,000	38,000		20
		$\bar{\bar{X}}$=37,000		81
III U_a	1,000 → 24,000	10,000	6,400	22
III U_b	1,000 → 26,000	11,600		22
III U_c	1,000 → 28,000	9,600		23
III U_d	1,000 → 22,000	8,600		23
		$\bar{\bar{X}}$-10,000		90

Table VI

Raw Talysurf Data (Divisions)

400Å/div.	1000Å/division				10,000Å/division				4000Å/division			
III F	III M_a	III M_b	III M_c	III M_d	III R_a	III R_b	III R_c	III R_d	III U_a	III U_b	III U_c	III U_d
data on following page	1 1/2	2	1 1/4	3/4	3 1/2	8	1/2	7 3/4	2	3 3/4	1/2	1 1/2
	1 1/2	1	3/4	1 3/4	4 1/2	1	3 1/2	7		1/4	2 1/2	2 1/4
	1	2 1/2	1/4	1/2	7	1/2	4 3/4	3 1/2	1/2	1/2	1	2 1/2
	1 1/2	1	1	2	7	3 1/2	3	2 1/2	1/4	1	7	3
	1	1/4	1	2	6 1/2	6 1/4	6 1/2	9	1 1/2	6	3	2 1/2
	1/2	2	3	1 1/4	4	5 1/2	9	2 3/4	2 3/4	1/2	1 3/4	1/4
	1/2	1 1/2	1	1/4	3	4 1/2	5	2 1/4	1 1/2	1/2	3 3/4	2 1/2
	3/4	1/2	1/2	1	3	6 1/4	3 1/2	4 1/2	5	2	1/2	1 1/4
	1 3/4	1 1/2	1/2	1/2	5 1/2	1 1/4	2	6 1/2	2 1/2	1 3/4	3 1/2	5
	1	1	1 1/2	1/2	1 1/2	2	1	4 1/2	1 3/4	3 1/4	2 3/4	5 1/2
	2 1/2	1/2	1 1/2	1	1	5	2 3/4	3 1/2	3 1/4	1 3/4	1/4	1 1/2
	1	3	1	1/4	3	2	3	4	6	3/4	4 1/4	1
	3/4	3 1/2	1	2	3	1	3	1 1/2	5 1/2	4 1/2	1/4	1 1/4
	1 3/4	1	2	2 1/2	1 1/2	3	2	1/2	2 3/4	1/2	1/4	2 3/4
	1/4	1 1/2	1	1/2	4	7	3 1/2	6	1/4	3 1/2	2 1/2	3 1/2
	1/2	1	1 1/2	1/2	5 1/2	4	53	7 1/4	3/4	5 1/2	4 3/4	2
	1 1/2	25	2	3/4	6	1		3 1/4	1 1/2	4	5 1/2	3
	1		1 1/2	1	1	61 3/4		7	4 1/2	6 1/2	1 1/2	3
	1		2	19	4 1/2			9	3	1	1	1/2
	21 1/4		24 1/4		5			9	3 1/2	2 3/4	3 1/2	1 1/4
					5 1/2			101 1/4	2 1/2	5	1 1/4	1 1/2
					4 1/2				1 1/4	4	2 3/4	1/4
					2 1/2				2 1/4	62 1/4	1	3
					1 1/2				54 3/4		55	50 3/4
					5							
					2 1/2							
					2 1/2							
					2							
					3							
					109							

III F Etching Region

X_i		$(X_i - \bar{X})$		$(X_i - \bar{X})^2$	
6	3 1/2	2.7	.2	7.29	.04
1 1/2	3	1.8	.3	3.24	.09
4	3 1/2	.7	.2	.49	.04
2 1/2	4 1/2	.8	1.2	.64	1.44
5	1 3/4	1.7	1.55	2.89	2.4
7	1/4	3.7	3.05	13.69	9.3
3	1 1/2	.3	1.8	.09	3.24
2	1 1/2	.7	1.8	.49	3.24
3 12/	2 1/4	.2	1.05	.04	1.11
4 1/2	1 1/2	1/2	1.8	1.44	3.24
6 1/2	4	3.2	.7	10.54	.49
6	3/4	2.7	2.55	7.29	6.5
3	5	.3	1.7	.09	2.89
5	2	1.7	1.3	2.89	1.69
4	3 1/4	.7	.05	.49	-
5 1/2	1 1/2	2.2	1.8	4.84	3.24
2 1/2	4 1/2	.8	1.2	.64	1.44
1	2 1/2	2.3	.8	5.29	.64
2 1/2	1 1/2	.8	1.8	.64	3.24
2 1/2	3	.8	.3	.64	.09
1 1/2	2	1.8	1.3	3.24	1.69
1	1 1/2	2.3	1.8	5.29	3.24
4	6	.7	2.7	.49	7.29
3	168.25	.3		.90	Σ 167.31
2		1.3		1.69	
4		.7		.49	
8		4.7		22.1	
7		3.7		13.69	

$$\bar{X} = \frac{168.25}{51} = 3.3$$

$$S = \sqrt{\frac{(X_i - \bar{X})^2}{n - 1}}$$

$$= \sqrt{\frac{167.31}{50}} = 1.83$$

III M_c Polishing Plateau

$\bar{X} = \frac{24.95}{19} = 1.275$

$(X_i - \bar{X})$	$(X_i - \bar{X})^2$
.025	.0006
.525	.276
1.025	1.05
.275	.0754
.275	.0754
1.725	2.8
1.275	1.63
.775	.6
.775	.6
.225	.051
.225	.051
.275	.0754
.275	.0754
.725	.525
.275	.0754
.225	.051
.725	.525
.225	.051
.725	.525
	Σ 9.1126

$$S = \sqrt{\frac{(X_i - \bar{X})^2}{n-1}} = \sqrt{\frac{9.1126}{18}} = 0.71$$

III R_b Slow Gas Evolution Region

$\bar{X} = \frac{61.75}{17} = 3.63 = 3\ 5/8$

$(X_i - \bar{X})$	$(X_i - \bar{X})^2$
4 3/8	1225/64
2 5/8	441/64
3 1/8	625/64
1/8	1/64
2 5/8	441/64
1 7/8	225/64
7/8	49/64
2 5/8	441/64
2 3/8	361/64
1 5/8	169/64
1 3/8	121/64
1 5/8	169/64
2 5/8	441/64
5/8	25/64
3 3/8	729/64
3/8	9/64
2 5/8	441/64
	$\sum$ 5913/64 = 92.5

$$S = \sqrt{\frac{(X_i - \bar{X})^2}{n - 1}} = \sqrt{\frac{92.5}{16}} = 2.38$$

III U_a Fast Gas Evolution Region

$\bar{X} = \frac{54.75}{22} = 2.49 = 2\ 1/2$

$(X_i - \bar{X})$	$(X_i - \bar{X})^2$
1/2	1/4
2	4
2 1/4	5 1/16
1	1
1/4	1/16
1	1
2 1/2	6 1/4
0	0
3/4	9/16
3/4	9/16
3 1/2	12 1/4
3	9
1/4	1/16
2 1/4	5 1/16
1 3/4	3 1/16
1	1
2	4
1/2	1/4
1	1
0	0
1 1/4	1 9/16
1/4	1/16
	Σ 54 1/16

$$S = \sqrt{\frac{(X_i - \bar{X})^2}{n - 1}}$$

$$= \sqrt{\frac{54\ 1/16}{21}} = 1.6$$

Figure 17. Distribution of surface profile values. ("LOOK TEST")

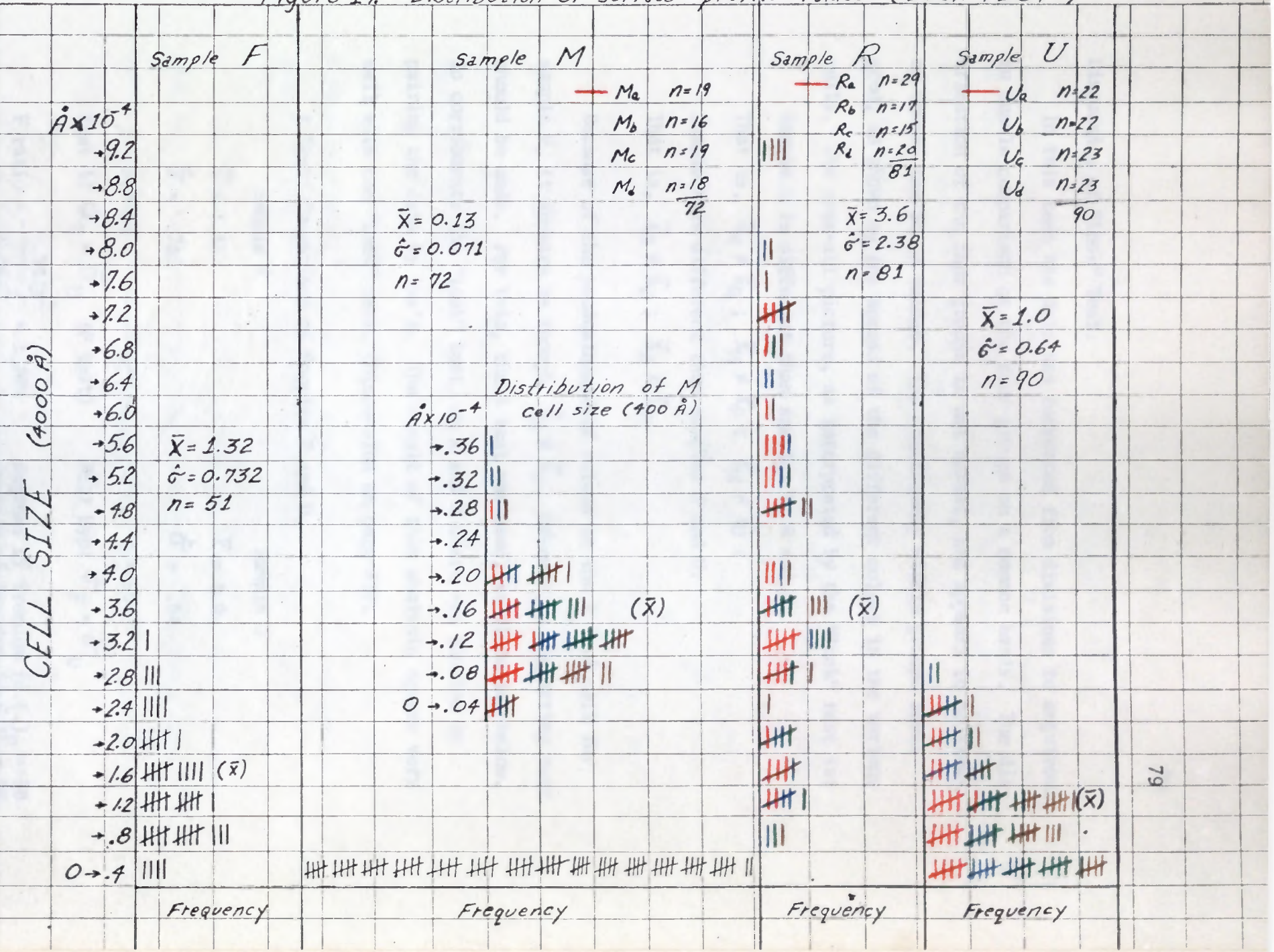

Discussion of "Look" Test.

In this test the data was converted from divisions to angstroms, to enable comparison of the four groups on a common basis. The distribution of the four groups is not normal, and appears to be skewed toward the lower values. The consistency within groups looks good, as shown by the spread of the different colors in the various cells. The over-all picture, as interpreted by the "look" test is:

Sample M is different than samples F, R and U.

That is, $\bar{X}_M \neq \bar{X}_R$; $\bar{X}_M \neq \bar{X}_F$; $\bar{X}_M \neq \bar{X}_U$.

Sample R is different than samples F and U.

That is, $\bar{X}_R \neq \bar{X}_F$; $\bar{X}_R \neq \bar{X}_U$.

Because of the predominance of values in the 0 → .4 cell for sample U, it appears as though $\bar{X}_U \neq \bar{X}_F$. However, a supporting test should be made. For this, the t test was used, as discussed below. To corroborate the "look" test, an $\bar{X}$ and R chart was plotted by pairing the data by two's. The result of this analysis agrees very well with the "look" test. (Discussion on page 85).

t Test: Comparison of Samples F and U.

Sample F	Sample U
$\bar{X} = 1.32$	$\bar{X} = 1.0$
$\hat{\sigma} = .732$	$\hat{\sigma} = .64$
$n = 51$	$n = 90$
Test if $\hat{\sigma}_F = \hat{\sigma}_U$ (F test)	Null Hyp: $\hat{\sigma}_F = \hat{\sigma}_U$
F ratio $= \frac{(.732)^2}{(.64)^2} = 1.306$	degrees of freedom $(d.f.)_F = 50$ degrees of freedom $(d.f.)_U = 89$

$F_{.05/50/89} = 1.46$ $\qquad$ $F_{.01/50/89} = 1.70$

Therefore one cannot reject the hypothesis, and as a result to test if $\bar{X}_F = \bar{X}_U$ you must use the t test for two populations having the same mean when σ^2 is not known.

Null Hyp: $\bar{X}_F = \bar{X}_U$

$$t = \frac{\bar{X}_F - \bar{X}_U}{S_p\sqrt{(1/N_F) + (1/N_U)}}$$

$$t = \frac{1.32 - 1.00}{.675\sqrt{1/51 + 1/90}}$$

$$t = \frac{.32}{.675 \times .175} = 2.71$$

d.f. = 139

Where $S_p^2 = \hat{\sigma}_p^2$, the pooled mean square estimate of σ^2, given by:

$$S_p^2 = \frac{(N_F - 1)\hat{\sigma}_F^2 + (N_U - 1)\hat{\sigma}_U^2}{N_F + N_U - 2}$$

$$S_p^2 = \frac{(50)\ (.732)^2 + (89)\ (.64)^2}{139}$$

$S_p^2 = .455, \qquad S_p = .675$

$t_{.95/120} = 1.658;$ $\qquad$ $t_{.995/120} = 2.617$

Therefore $\bar{X}_F \neq \bar{X}_U$ (i.e. reject hypothesis)

The results of the t test show that you can say $\bar{X}_F \neq \bar{X}_U$ with a 99.5% confidence. This high degree of confidence is not readily seen by looking at the two distributions (see "look" test).

The strength of this test lies in the large number of samples that make up the populations, because the t test is actually comparing the distribution of the <u>averages</u> making up the two populations. That is:

$\hat{\sigma}_p = .675$ (estimate of the universe standard deviation).

$\hat{\sigma}_{\bar{X}} = (.675)(.175) = .12$ (estimate of the standard deviation of the averages).

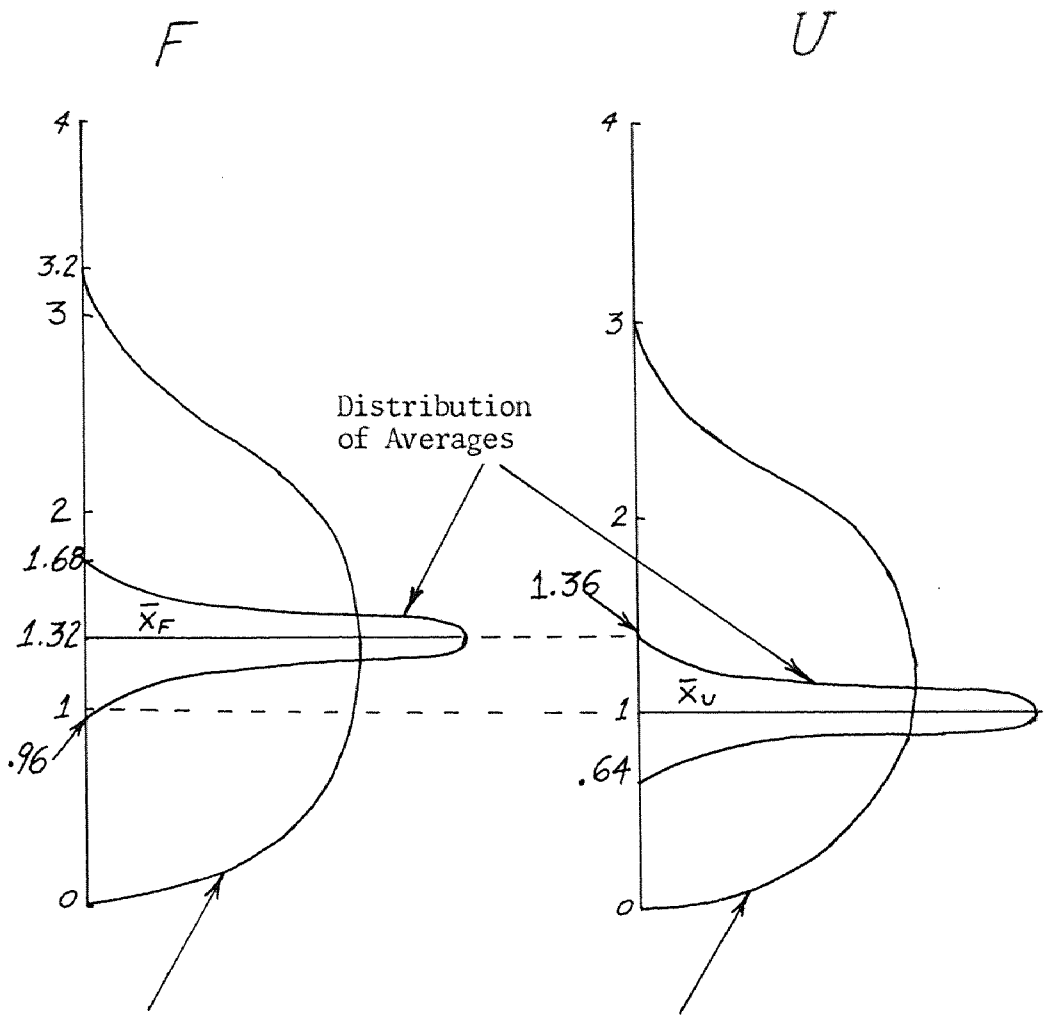

Skewed distribution of samples from F population.

Skewed distribution of samples from U population.

Therefore: $\bar{X}_F = 1.32$, $\bar{X}_U = 1.00$, and $3\hat{\sigma}_{\bar{X}} = .36$

The sketch presented above dramatically illustrates the conclusion $\bar{X}_F \neq \bar{X}_U$.

Table VII

Data for $\bar{X}$ and Range (R) Chart; (Arbitrarily paired adjacent values), Readings in $\mathring{A} \times 10^{-4}$

Sample F		Sample M				Sample R				Sample U			
$\bar{X}$	R	$\bar{X}$	R	$\bar{X}$	R	$\bar{X}$	R	$\bar{X}$	R	$\bar{X}$	R	$\bar{X}$	R
1.5	1.8	.15	0	.125	.10	4.0	1.0	4.25	1.5	.7	.6	.9	1.6
1.3	.6	.125	.05	.125	.15	7.0	0	1.5	1.0	.35	.5	.1	0
2.4	.8	.075	.05	.163	.075	5.25	2.5	2.875	.25	.85	.5	1.45	.9
1.0	.4	.063	.025	.063	.075	3.0	0	5.625	$4.25\text{-}R_c$	1.0	.6	.9	1.0
1.6	.4	.138	.075	.05	0	3.5	4.0	5.25	3.5	2.3	.2	.8	.6
2.5	.2	.175	.15	.063	.075	2.0	2.0	5.75	6.5	.6	1.0	.5	$.2\text{-}U_c$
2.5	.8	.125	.10	.225	.05	2.75	1.5	2.5	.5	.45	.3	.95	.1
1.9	.6	.038	.025	.05	0	4.75	1.5	5.5	2.0	1.5	.6	1.1	.2
.7	.6	.125	.05	.088	$.025\text{-}M_d$	3.5	5.0	3.75	.5	1.2	.4	.55	.9
1.0	0	.15	$.10\text{-}M_a$			4.75	1.5	1.0	1.0	.7	$.4\text{-}U_a$	1.25	1.5
.5	.2	.175	.15			4.75	1.5	6.625	1.25	.8	1.4	1.4	1.6
1.4	.4	.113	.175			2.0	1.0	5.125	3.75	.3	.2	.45	.1
1.2	.8	.10	.10			3.75	2.5	9.0	$0\ \text{-}R_d$	1.3	2.2	1.25	.3
3.0	.4	.075	.05			2.25	.5			.5	.6	1.0	.4
1.3	.2	.313	.05			5.5	$5.0\text{-}R_a$			1.0	.6	.7	1.0
1.6	.4	.125	.05			.75	.5			.5	.4	.45	.1
.4	.6	.113	$.025\text{-}M_b$			4.875	2.75			1.0	1.6	.65	$.1\text{-}U_d$
.6	0	.05	.05			5.0	1.0			2.2	.8		
.75	.3	.10	0			3.75	5.0			2.1	1.0		
.95	1.3	.20	.20			3.5	3.0			.75	.7		
1.4	1.2	.05	0			1.5	1.0			1.8	.4		
.95	.7	.15	0			5.0	4.0			.6	$.4\text{-}U_b$		
1.4	.8	.10	0			2.5	$3.0\text{-}R_b$			1.6	2.4		
.9	.6	.15	.10			2.0	3.0			.95	.5		
.7	.2	.175	$.05\text{-}M_c$			3.875	1.75			.25	.1		
						7.75	2.5			1.25	.3		

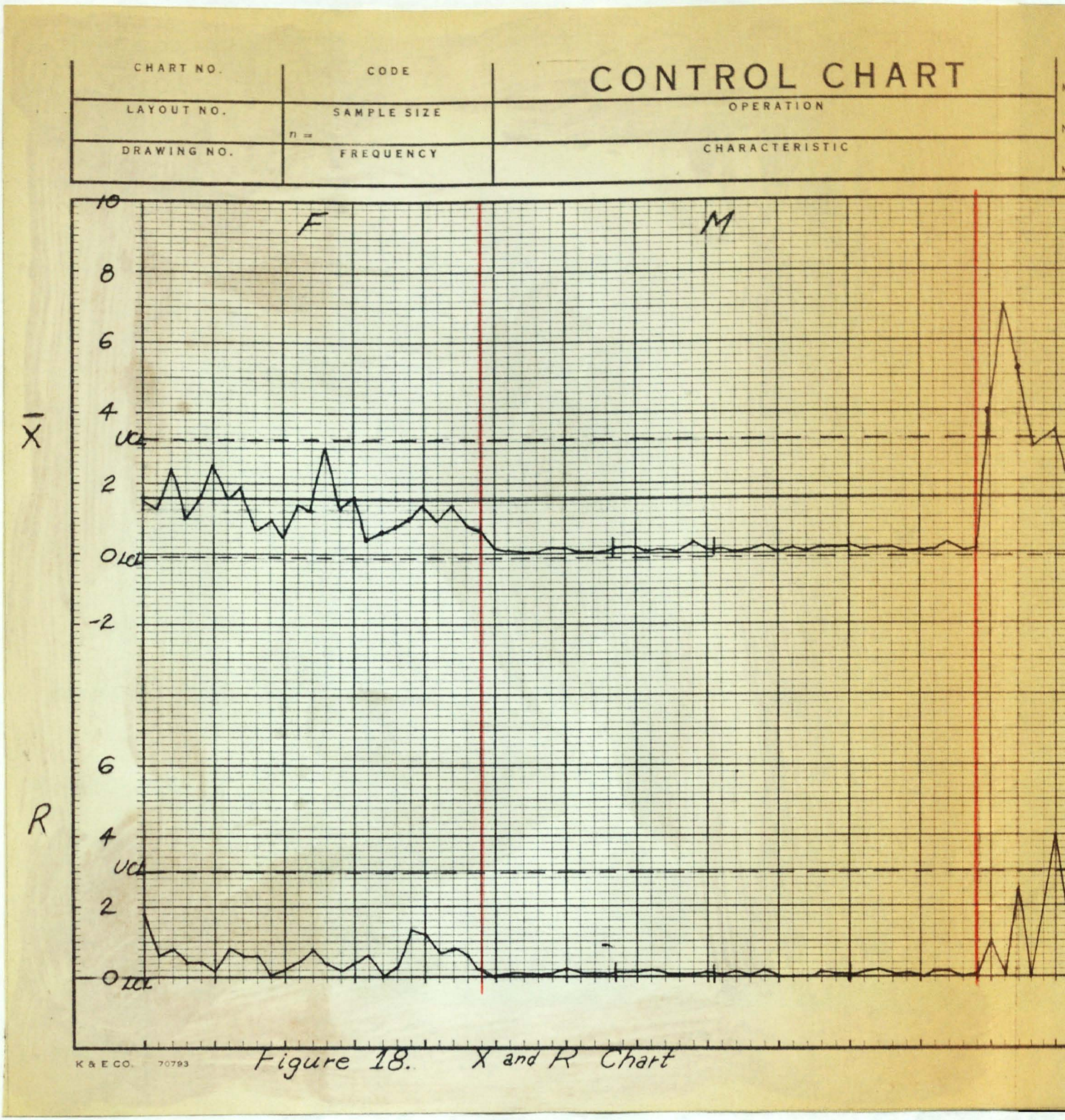

Figure 18. X and R Chart

CHART

SPECIFICATION	DEPARTMENT	PART NO.	CODE	CONTROL CHART
MAX:				
NOM:	MACHINE NO.	YOUT NO.	SAMPLE SIZE $n =$	OPERATION
MIN:	APPROVED BY	AWING NO.	FREQUENCY	CHARACTERISTIC

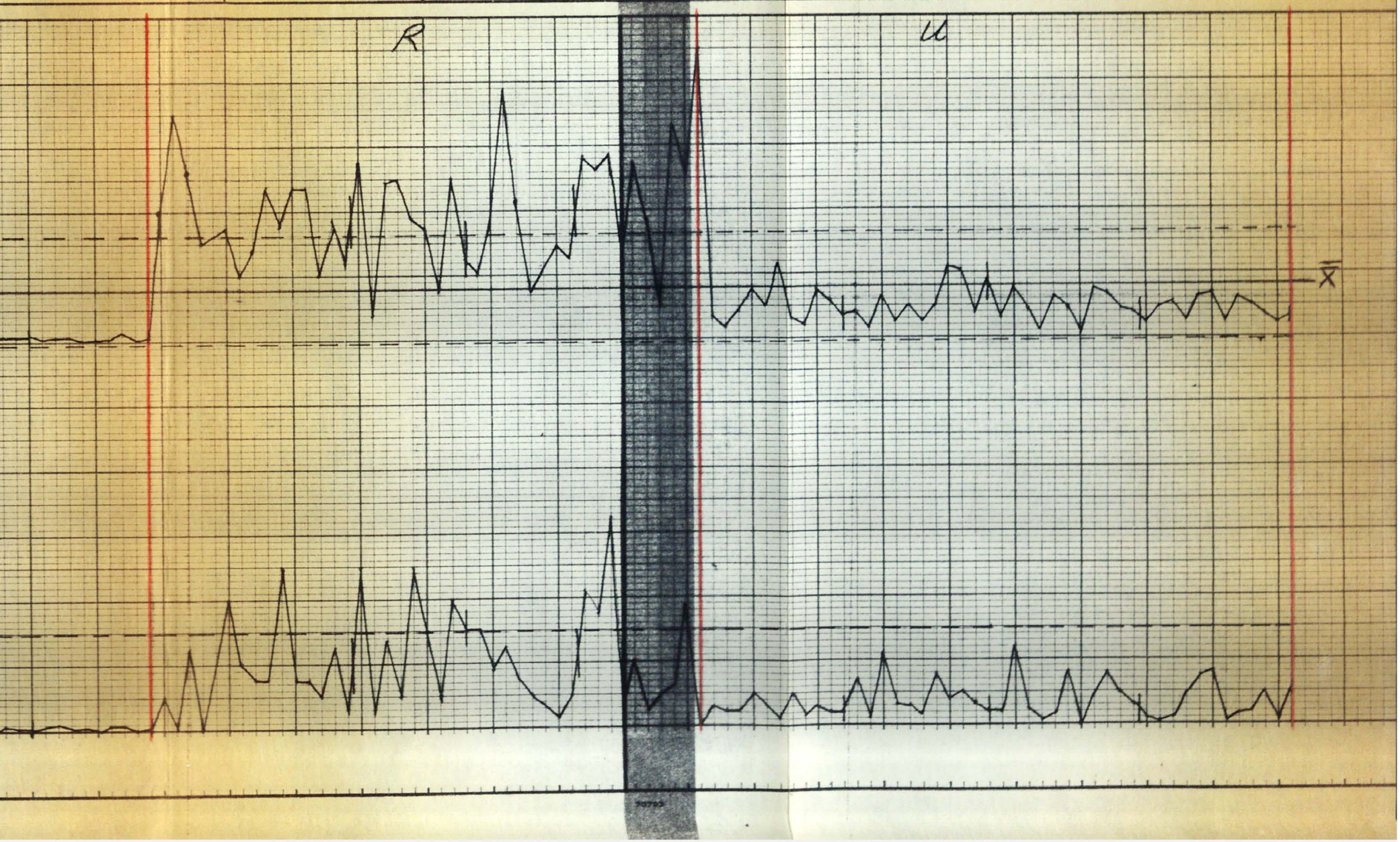

Calculation of Upper and Lower Control Limits for X and R Chart.

$$\bar{\bar{X}} = \frac{\bar{X}}{n} = \frac{238.87}{147} \qquad \text{Where } n = \frac{n_F + n_M + n_R + n_U}{2} = \frac{294}{2} = 147$$

$$\bar{\bar{X}} = 1.625$$

$$\bar{R} = \frac{R}{n} = \frac{133.425}{147} = .908$$

$\bar{X}$	R
$UCL = \bar{\bar{X}} + A_2\bar{R}$	$UCL = D_4\bar{R}$
$= \bar{\bar{X}} + 1.88\bar{R}$	$= 3.27\ \bar{R}$
$= 1.625 + 1.88(.908)$	$= 3.27(.908)$
$= 3.33$	$= 2.97$
$LCL = \bar{\bar{X}} - 1.88\ \bar{R}$	$LCL = D_3\bar{R}$
$= 1.625 - 1.707$	$= 0(R)$
$= -.082$	$= 0$

Discussion of Results From $\bar{X}$ and R Chart.

By examining the $\bar{X}$ and R chart, the conclusions drawn support those made using the "look" test. Actually this analysis is very similar to the look test. It is seen that the consistency within groups is good. An immediate set of conclusions from this chart are:

$$\bar{X}_F \neq \bar{X}_M \; ; \quad \bar{X}_F \neq \bar{X}_R \; ; \quad \bar{X}_M \neq \bar{X}_R \; ; \quad \bar{X}_R \neq \bar{X}_U \; ; \quad \bar{X}_M \neq \bar{X}_U$$

To say that $\bar{X}_F \neq \bar{X}_U$ requires some additional analysis. Observe that there are nine consecutive points in population F, that fall below $\bar{\bar{X}}$. If the populations of all the groups were assumed to be

from one population, then according to probability you would expect 1/2 the points to fall above $\bar{\bar{X}}$ and 1/2 to be below $\bar{\bar{X}}$. Thus getting 9 consecutive points below $\bar{\bar{X}}$ results in a probability of $Pr\ (1/2)^9$. For the U population there are 21 consecutive points below $\bar{\bar{X}}$, resulting in a probability of $Pr\ (1/2)^{21}$. Therefore, one may conclude that $\bar{X}_F \neq \bar{X}_U$.

The Wald-Wolfowitz Runs Test.[25]

Data For Runs Test Between Samples F & M.

five		1/4	- M	
seven		1/2	- M	
five		3/4	- M	
twenty	1		- M	M
one	1		- F	F
two	1	1/4	- M	M
eleven	1	1/2	- M	
three	1	3/4	- M	
eight	2		- M	
three	2	1/2	- M	M
two	3		- M	M
one	3		- F	F
one	3	1/2	- M	M
forty-nine	> 3	1/2	- F	

Total = one hundred and twenty-three (72 - M, 51 - F)

U = # of runs = 6 (minimum); = 6 (maximum)

N_1= 72 (samples of M)

N_2= 51 (samples of F)

$$U_u = \frac{2N_1N_2}{N_1+N_2} + 1 = \frac{2(72)(51)}{123} + 1 = 60.7$$

$$\sigma_u^2 = \frac{2N_1N_2(2N_1N_2 - N_1 - N_2)}{(N_1 + N_2)^2(N_1 + N_2 - 1)} = \frac{(7344)(7221)}{(123)^2(122)} = 28.73$$

$$\sigma_u = 5.36$$

Siegel[25] in his book Non-Parametric Statistics suggests if ties occur, you should break the ties in all possible ways and observe the resulting value for the # of runs, and thereby determine the significance of these ties. Therefore:

minimum # of runs = 6 (treating ties as tabulated)	maximum # of runs = 6 (since only one F value was associated with each tie).

Thus, in this case the two ties don't affect the # of runs.

$$Z = \frac{U - U_u + 1/2}{\sigma_u} = \frac{6 - 60.7 + 1/2}{5.36} = -10.1$$

Therefore: Can say that $\bar{X}_M \neq \bar{X}_F$ with a 99.9% confidence. This result supports the "look" test and $\bar{X}$ and R chart results.

Data For Runs Test Between Samples M & U.

seventeen	1	- M	
twenty	1	- M	
eight	1	- U	
two	1	1/4 - M	
eleven	1	1/2 - M	
three	1	3/4 - M	
eight	2	- M	Total = one hundred and sixty-two
eight	2	- U	
three	2	1/2 - M	(72 - M, 90 - U)
two	3	- M	
three	3	- U	
one	3	1/2 - M	
all the rest are		- U	

U = minimum # of runs = 8

N_1 = 72 (samples of M)

N_2 = 90 (samples of U)

Substituting these values into the formulas given on page 86 gives:

$$U_u = 81$$

$$\sigma_u = 6.273$$

Thus for the minimum # of runs;

$$Z = \frac{U - U_u + 1/2}{\sigma_u} = \frac{8 - 81 + 1/2}{6.273} = -11.5$$

Therefore: Can say that $\bar{X}_M \neq \bar{X}_U$ with a greater than 99.9% confidence.

When U = maximum # of runs = 40,

$$Z = \frac{U - U_u + 1/2}{\sigma_u} = \frac{40 - 81 + 1/2}{6.273} = -6.5$$

Thus by calculating the maximum number of runs, and therefore in this case the minimum Z, you can still say that $\bar{X}_M \neq \bar{X}_U$ with a greater than 99.9% confidence.

Data For Runs Test Between Samples R & U.

eight	1/4	- U	four	3 3/4	- R
eight	1/2	- U	two	4	- U
three	3/4	- U	one	4 1/4	- U
six	1	- U	two	4 1/2	- U
five	1 1/4	- U	one	4 3/4	- U
three	1 1/4	- R	three	5	- U
five	1 1/2	- U	five	5	- R
four	1 3/4	- U	four	5 1/2	- U
three	2	- U	one	5 5/8	- R
two	2 1/4	- U	two	6	- U
seven	2 1/2	- U	three	6 1/4	- R
six	2 1/2	- R	one	6 1/2	- U
six	2 3/4	- U	two	6 7/8	- R
six	3	- U	one	7	- U
one	3 1/8	- R	fifty-four	7	- R
two	3 1/4	- U			
five	3 1/2	- U			
one	3 3/4	- U			

Total = one hundred & seventy-one

(90 - U, 81 - R)

U = minimum # of runs = 18

N_1 = 90 (samples of U)

N_2 = 81 (samples of R)

Substituting these values into the formulas given on page 86 gives:

$$U_u = 86.3$$

$$\sigma_u = 6.50$$

Thus for the minimum # of runs;

$$Z = \frac{U - U_u + 1/2}{\sigma_u} = \frac{18 - 86.3 + 1/2}{6.50} = -10.43$$

Therefore: Can say that $\bar{X}_R \neq \bar{X}_U$ with a greater than 99.9% confidence.

When U = maximum # Of runs = 40,

$$Z = \frac{U - U_u + 1/2}{\sigma_u} = \frac{40 - 86.3 + 1/2}{6.50} = -7.05$$

Thus by calculating the maximum # of runs, and therefore the minimum Z, you can still say that $\bar{X}_R \neq \bar{X}_U$ with a greater than 99.9% confidence.

It is expected that similar results would be obtained if the runs test was used between samples F and R. However, in the case of samples F and U the runs test is not appropriate because of the many ties. That is, Z would go from one extreme to the other (-→+), and as Siegel[25] points out, if the various possible ways of breaking up ties leads to some values of U(#of runs) which are significant and some which are not, the decision as to accepting or rejecting H_o (the hypothesis) is difficult; and if the # of ties is very large, than U is essentially indeterminate.

Library
Newark College of Engineering
56440

IV CONCLUSIONS

1. As a result of this experiment, four types of surface finishes can be obtained for copper and nickel silver, which will facilitate the study of the effect of surface condition on ultrasonic weldability. These four surfaces are characterized by an etched, polished, pitted, and polished with a slight pitted appearance. They result from operating in the etching region, polishing plateau, slow gas evolution region and fast gas evolution region respectively, on the anode current density versus voltage curve obtained for a given system.

2. The existence of the anode viscous layer and anode surface film was verified, and their role in the polishing process was found to support the current electrolytic polishing theory. Based on the observations made during the course of this experiment, the most general mechanism to explain the polishing process is in support of the diffusion mechanism discussed in section I.

3. Statistical analysis of the data for the Cu/H_3PO_4 system disclosed that the four surfaces obtained were significantly different, and good reproducibility of the surfaces could be achieved. The regression analysis performed on the data for the anode current density versus voltage curve

indicated that the curve obtained was in close agreement with that predicted by electropolishing theory.

4. For the nickel silver - phosphoric acid system, deburring can be accomplished by operating in the fast gas evolution region. The application of an electrodeburring procedure during the manufacture of nickel silver contact springs at Western Electric Company, Kearny Works has been proposed. However, for various reasons, not known to the author, it has not been put into production.

V FURTHER AREAS OF STUDY

The literature review presented in an earlier section, plus the present study are indicative of the appreciable experimental work which has been performed with the Cu/H_3PO_4 system. Consequently much of the results which have been obtained are of an empirical nature. However there are still many loopholes in the electropolishing theory and the need for a mechanism more amenable to generalization has yet to be proposed. Along these lines, the application of the electron microscope and the electron beam microprobe would be valuable tools for a study of this magnitude. They could be used for visual observation and quantitative chemical analysis of the anode viscous layer and anode surface film. A more recent entry into the field of electron beam technology has been the scanning electron microscope. Because of the high depth of field and resolution, this instrument is capable of giving micrographs at up to 30,000X which have a three dimensional quality. The surface topography is shown in microscopic detail by using the Thornley-Everhart[29] secondary electron collector, which is basically a scintillator and photomultiplier. The signal from the photomultiplier is converted to a voltage, amplified and used to control the brilliance of a cathode ray tube whose electron beam is moved in synchronism with the primary beam of the specimen. The CRT thus presents an image in terms of secondary electron emission of the surface topography of the specimen. A significant advantage of the scanning electron micro-

scope relative to the electron microscope is the ease of sample preparation. Actually the specimens prepared for the current study could be viewed with the SEM without further specimen preparation.

Thus far general comments have been made suggesting the application of electron beam technology to study electrolytic polishing phemonena. Some specific areas which may add to the knowledge of electrolytic polishing processes are listed below:

1. Application of radioactive isotopes, with an immersible probe to study diffusion in the anode viscous layer. The experimental problems associated with this technique are quite formidable, however it could lead to a quantitative approach to the diffusion mechanism.
2. A thermodynamical approach to determine the energies associated with the anode viscous layer and anode surface film and the barriers they offer to diffusion.
3. The effect of the various polishing parameters on the surfaces obtain for various alloys, and their effect on the polishing equilibrium.
4. The effect of surface states on the polishing process. The use of semiconductor materials such as silicon and germanium is suggested, since there is considerable data available in the literature for these elements. Areas to be considered in a study of this nature are: dislocation density and distribution, impurity concentration, single crystal or polycrystalline and orientation.

Because of the concept of this section, the ideas presented above must be of a general nature. However, it is hoped that the basic ideas expressed will be of some value to the reader interested in broadening the knowledge of electrolytic polishing processes.

VI REFERENCES

1. P. A. Jacquet, "Electrolytic and Chemical Polishing." Met. Rev. 1, Part 2, 157-238 (1956).

2. D. Laforgue - Kantzer, "On the Electrolysis of Phosphoric Acid Between Copper Electrodes." Compt. Rend. 233,547 (1951).

3. W. J. M. Tegart, Electrolytic and Chemical Polishing, (1956) Pergamon Press.

4. P. A. Jacquet, "On the Electrolytic Polishing of Copper, Lead, Tin and Their Alloys and its Application to Metallography." Bull. Soc. Chim. Franc. 3, 705 (1936).

5. H. F. Walton, "The Anode Layer in the Electrolytic Polishing of Copper." J. Electrochem. Soc. 97, 219 (1950).

6. M. Halfawy, "Experientia 7, 175 (1951).

7. T. P. Hoar and T. W. Farthing, "Solid Films on Electropolishing Anodes." Nature 169, 324 (1952).

8. L. Meunier, "On the Dynamic Functioning of a Cell for the Electrolytic Polsihing of Copper." Comptes Rendues de II Reunion, Milan, P. 242 (1950).

9. H. Lal, "The Nature of the Electropolishing State." Sym. on Elec. Plat. and Met. Fin. (Nat. Met. Lab. - India) 54, (1952).

10. W. C. Elmore, "Electrolytic Polishing." J. Appl. Phys. 10, 724 (1939).

11. W. C. Elmore, "Electrolytic Polishing." J. Appl. Phys. 11, 797 (1940).

12. J. Edwards, "Phosphoric Acid Solutions, Processess Preceding the Establishment of Polishing Conditions." J. Electrochem. Soc. 100, 189C (1953).

13. J. Edwards, "Phosphoric Acid Solutions, the Mechanism of Smoothing." J. Electrochem. Soc. 100, 223C (1953).

14. C. Wagner, "Contributions to the Theory of Electropolishing." J. Electrochem. Soc. 101, 225 (1954).

15. U. R. Evans and D. Whitwham, "Note of a Convenient Method of Electropolishing Aluminum Alloys." J. Electrodep. Tech. Soc. 22, 24 (1947).

16. E. Darmois and D. Amine, Compt. Rend. 237, 501 (1953).

17. G. S. Vozdvizhensky, Zhur, Tekhn. Fiziki 18, 403 (1948).

18. J. Mercadie, Compt. Rend. 226, 1450, 1519 (1948).

19. E. Kmuth-Winterfeldt, Arch. Eisenhuttenwesen 25, 393 (1954).

20. P. Michel, "Recent Research in Electrolytic Polishing." Sheet Met. Ind. 26, 2175 (1949).

21. R. W. K. Honeycombe & R. R. Hughen, "Electrolytic Polishing of Copper in Orthophosphoric Acid." J. Council Sci. Ind. Res. (Aust.) 20, 297 (1947).

22. A. Hickling and J. K. Higgins, "The Rate Determining Stage in the Anodic Dissolution of Metals." Trans. Inst. Met. Finishing 29, 274 (1953).

23. J. N. Agar and T. P. Hoar, "The Influence of Change of Size in Electrochemical Systems." Faraday Soc. Discuss. "Electrode Processes." 158 (1947).

24. T. P. Hoar and J. A. S. Mowat, "Mechanism of Electropolishing." Nature 165, 64 (1950).

25. Siegel, Non-Parametric Statistics, (1956) McGraw-Hill.

26. C. L. Faust, U. S. Patent 2,334,699.

27. C. L. Faust, U. S. Patent 2,429,676.

28. C. L. Faust, U. S. Patent 2,440,715.

29. R. F. M. Thornley and T. E. Everhart, "Wide-band Detector For Micro-microampere Low-energy Electron Currents." J. of Sci. Inst. 37, 246-248 (1960).